DEGREE PROJECT IN TECHNOLOGY,
SECOND CYCLE, 30 CREDITS
STOCKHOLM, *SWEDEN 2021*

Performance Investigation & Gas Exchange Assessment of Exhaust Piston–assisted Turbocharged Engine (EPTE) Concept

A simulation-based assessment

NACHIKETH LINGACHARI ACHARYA & SAURAV DASGUPTA

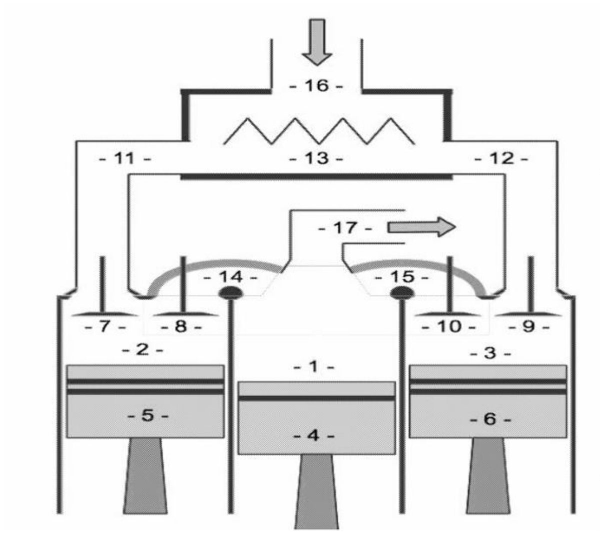

Master of Science Thesis TRITA-ITM-EX 2021:546
KTH Industrial Engineering and Management
Machine Design, Division of Internal Combustion Engines
SE-10044 STOCKHOLM

KTH Industriell teknik
och management

Examensarbete TRITA-ITM-EX 2021:546

Analys av prestanda och bedömning av gasutbyte för koncept med avgaskolv som assisterar turboladdning av motor (EPTE)

Simuleringsbaserad bedömning

Nachiketh Lingachari Acharya
Saurav Dasgupta

Godkänt	Examinator	Handledare
2021-09-18	Andreas Cronhjort *andreas.cronhjort@itm.kth.se*	Andreas Cronhjort *andreas.cronhjort@itm.kth.se*
	Uppdragsgivare Olshammar Nebula AB	Kontaktperson Mats Olshammar *mats@olshammar.se*

Sammanfattning

Ökade krav i lagstiftningen för utsläpp inom transportindustrin, tillsammans med ambitiösa krav på effekt och bränsleekonomi från kundsidan, har drivit fordonstillverkarna och relevanta leverantörer av komponenter att utveckla och integrera en bred portfölj av motorteknik. Turboladdning är en sådan teknisk lösning som används av industrin för att minska bränsleförbrukningen och därmed koldioxidutsläpp från avgasröret. Området inom vilket turboladdning har praktiserats sträcker sig över en mängd olika fordonssegment, för både vägtrafik och offroad-applikationer.

Det är välkänt att standard turboladdning har en nackdel, då den inte har förmågan att tillhandahålla god effektivitet över ett brett driftsområde. Dessutom har fyrtaktsmotorer med få cylindrar ojämna avgaspulser som strömmar in i turbons turbin. Detta gör att turbon inte klarar systemets krav på lufttillgång under motorns hela cykeln. Det finns befintliga kommersiella teknologier som turboladdning med ”twin-scroll”, turbo med variabel geometri (VGT) och elektriskt assisterad turbo (EAT) för att hantera ovanstående utmaningar. Men de medför höga kostnader och övergripande systemkomplexitet. Ett patenterat konceptet, även kallat EPTE (Exhaust Piston-assisted Turbocharged Engine), hävdar att det adresserar dessa nackdelar med olika strategier för turboladdning. EPTE-konceptet använder en extra kolv och cylinder, som enbart komprimerar och expanderar de avgaser som kommer från förbränningscylindrarna. Denna extra kolv och cylinder kallas även EXC (Exhaust Cylinder).

Denna avhandling undersöker EPTE-konceptets prestanda och gasutbyte över ett brett motorvarvtal, och jämför detta med en basmotor som saknar EXC-komponenten. Utvärdering görs för att bedöma effekten av EXC-komponenten på turbon prestanda, samt dimensionering av ljuddämparen och system för efterbehandling av avgaser. Prestandaanalys har utförd för EXC-komponenten för att kvantifiera dess bidrag till den totala bromseffekten som produceras vid vevaxeln. Undersökningen utfördes med hjälp av det kommersiella verktyget för motorprestanda, GT-Power^{TM}. Ytterligare resultat av studien inkluderade utvärdering av fluktuationer i NBT (Normalized Brake Torque) och de fysiska förändringar på insugs- och avgassidan som krävs när basmotorn byggs om till EPTE. En utvärdering av specifikationerna för EXC-komponenten görs också i denna avhandling, för att ge en överblick över den extra kolven och cylindern från konstruktionssynpunkt.

EPTE-konceptet visade sig vara mer bränsleeffektivt och gav samtidigt högre effekt än basmotorn, när laddtrycket hade ett högt satt värde för begränsning av trycket. Det nya konceptet uppvisade nackdelar gällande bränsleeffektivitet och effekt vid lågt laddtryck. Konceptet visade sig också öka turbons prestanda genom att ge turbinen ett jämnare avgasflöde/tryck över motorns hela cykel, detta jämfört med basmotorn. Konceptet hade också en positiv inverkan på ljuddämpare och system för efterbehandling av avgaser, samt för storleken på motorns svänghjul, då alla dessa komponenter kunde minskas i dimension. Det observerades också att EPTE-konceptet kan ge dessa fördelar utan att behov av stora modifieringar av insugs- och avgassidans geometriska parametrar. Med en mindre turboladdare visade sig en sådan motor vara fördelaktig, jämfört med basmotorn, över hela motorns varvtalsregister.

Avhandlingen ger ett simuleringsbaserat perspektiv på systemnivå av EPTE-konceptet, som har patenterats av Mats Olshammar. Ett sådant perspektiv på systemnivå bidrar till en förståelse för EPTE innan man påbörjar några initiativ för utveckling av hårdvara. Rapporten ger också några rekommendationer för framtida arbete, baserade på de fördelar och nackdelar som konceptmotorn uppvisar i detta arbete.

KTH Industrial Engineering and Management	**Master of Science Thesis TRITA-ITM-EX 2021:546** **Performance Investigation & Gas Exchange Assessment of Exhaust Piston-assisted Turbocharged Engine (EPTE) Concept** *A simulation-based assessment* Nachiketh Lingachari Acharya Saurav Dasgupta

Approved	Examiner	Supervisor
2021-09-18	Andreas Cronhjort *andreas.cronhjort@itm.kth.se*	Andreas Cronhjort *andreas.cronhjort@itm.kth.se*
	Commissioner Olshammar Nebula AB	Contact person Mats Olshammar *mats@olshammar.se*

Abstract

There is an increasing stringency in the emission legislation within the transport industry along with ambitious performance demands from the customer side. These have pushed the vehicle manufacturers and relevant component suppliers to develop and integrate a wide portfolio of engine technologies. Turbocharging is one such technical solution deployed by the industry to reduce fuel consumption and thereby CO_2 emissions from the tailpipe. The area within which turbocharging has been practiced spans across a variety of vehicle segments including on-road and off-road applications.

It has been well established that standard turbocharging comes with a downside of not having the ability to provide suitable efficiency levels across a broad operating range. Furthermore, four-stroke turbocharged engines with fewer cylinders have uneven exhaust pulsations flowing into the turbine inlet. This implies that the turbocharger is not able to meet the air system demands throughout the engine cycle. There are existing commercial technologies such as twin-scroll turbocharging, Variable Geometry Turbochargers (VGTs) and Electrically-assisted Turbochargers (EAT) to tackle the above highlighted challenges. However, they induce high cost and overall system complexity. A patented concept also referred to as the Exhaust Piston-assisted Turbocharged Engine (EPTE) claims to address the aforementioned drawbacks related to various turbocharging strategies. The EPTE concept uses an extra piston-cylinder which acts solely as a compressor and expander for the exhaust gases flushing out of the combustion cylinders. This extra piston-cylinder is also referred to as the Exhaust Cylinder (EXC) component.

This thesis investigates the performance and gas exchange metrics of the EPTE concept across a broad engine speed range, and further compares those against a baseline engine which does not incorporate the EXC component. Gas exchange metrics were evaluated to assess the impact of the EXC component on the performance of turbocharger and sizing of the muffler and aftertreatment system. Performance analysis was conducted for the EXC component to quantify its contribution to the total brake power produced at the crankshaft. The investigation was performed using the commercial engine performance prediction tool, GT-Power^{TM}. Additional outcomes of the study included evaluation of Normalized Brake Torque (NBT) fluctuation and the hardware modifications in the intake and exhaust side required while transitioning from baseline engine to EPTE. An evaluation of the EXC component specifications was also conducted in this thesis to provide an overview of the extra piston-cylinder from the design standpoint.

The EPTE concept proved to be more fuel efficient while producing higher power output than the baseline engine at high boost pressure limits. The new concept exhibited disadvantages from the fuel efficiency and power output standpoint at low boost pressure limits. The concept proved to also increase the performance of the turbocharger by providing a smoother exhaust pressure pulse to the turbine across the engine cycle, when compared against the baseline engine. Furthermore, it had a positive impact on the aftertreatment sizing and flywheel inertia. Another observation was that the EPTE concept can produce such benefits while not having the need to radically modify the intake and exhaust geometrical parameters. With a smaller turbocharger, such an engine proved to be beneficial compared to the baseline engine across the whole engine operating range.

The thesis project provides a simulation-based system-level perspective of the EPTE concept which has been patented by Mats Olshammar. Such a system-level perspective will help to gain an understanding of the operation of the EPTE before commencing any hardware development initiatives. The report also provides some recommendations for future work, based on the advantages and disadvantages of the engine concept emanating from the results of the work.

Foreword

We would like to extend our gratitude to Mats Olshammar who served as our technical supervisor during this thesis project. We feel grateful to have worked under him in such an interesting proposition. His open mindedness gave us considerable amount of time to understand the stakeholders' requirements and potential demands pertaining to the patented engine concept. His high flexibility in coordination and communication provided us with a platform where we could contact him during challenging times and receive a fruitful feedback to meet the project goals.

We would also like to thank our master thesis examiner, Andreas Cronhjort, who first introduced us to the thesis project which Mats Olshammar had proposed. In addition to this, our thesis examiner continuously supported us with all the administrative aspects directly and indirectly related to the degree project. His honest feedback during particular stages of the project helped us to self-reflect on our work, which further improved the overall engineering content of the simulation approach and thesis report.

Furthermore, we would like to extend our gratitude to the customer support team from Gamma Technologies that supported us with technical queries related to the software GT-Power $^{\mathrm{TM}}$. The team's swift assistance provided us with the knowledge required to deploy suitable modelling choices for striking an optimal balance between computational time and internal validity.

Last but not the least, we would like to thank the IT-Support Team at KTH Royal Institute of Technology for helping us combat challenges related to system and network related aspects, and PhD researchers in the Internal Combustion Engine (ICE) division at KTH for providing us with introductory lessons regarding engine simulations.

Nachiketh Lingachari Acharya & Saurav Dasgupta

Stockholm, September 2021

Table of Contents

List of Abbreviations

BP	Brake Power
DOE	Design of Experiments
IDO	Integrated Design Optimizer
SI	Spark-Ignition
CI	Compression-Ignition
EGR	Exhaust Gas Recirculation
TDC	Top-Dead-Center
VGTs	Variable Geometry Turbochargers
BDC	Bottom-Dead-Center
RPM	Revolutions Per Minute
EIVC	Early Inlet Valve Closing
LIVC	Late Inlet Valve Closing
VVT	Variable Valve Timing
IVC	Inlet Valve Closing
EPA	Environmental Protection Agency
BMEP	Brake Mean Effective Pressure
EFIS	Electric Forced Induction System
EAT	Electrically-Assisted Turbocharger
LP	Low-Pressure
HP	High-Pressure
CAD	Crank Angle Degrees
EEVC	Early Exhaust Valve Closing
LEVC	Late Exhaust Valve Closing
EXC	Exhaust Cylinder
EPTE	Exhaust Piston-assisted Turbocharged Engine
OEMs	Original Equipment Manufacturers
ICE	Internal Combustion Engine
BSFC	Brake Specific Fuel Consumption
CMAES	Covariance Matrix Adaptation Evolution Strategy
PV	Pressure-Volume
PFI	Port Fuel Injected
FMEP	Friction Mean Effective Pressure
SOC	Start Of Combustion
TDCF	Top-Dead-Center Firing

List of Figures

List of Tables

Chapter 1

Introduction

This chapter includes the background of the project, research questions identified, purpose, stakeholders involved, delimitations and limitations, research approach adopted and the outline of the thesis report.

1.1 Background

This master thesis project has been performed in collaboration with Olshammar Nebula AB and KTH Royal Institute of Technology. Olshammar Nebula AB is a patent holding company owned by Mats Olshammar, a Swedish inventor. The inventor applied for a patent for his proposed engine concept in 2018, which got approved a year later. The engine concept was proposed based on the motive of increasing the fuel efficiency and performance of turbocharged engines. The concept engine has been predominantly named after the inventor as ”Olshammar Engine” [27]. However, to facilitate the ease of scientific understanding and disseminating technical know-how of the concept, it will be referred as Exhaust Piston-assisted Turbocharged Engine (EPTE) in the remaining portion of the document. The engine concept advocates the usage of an extra cylinder in addition to the firing combustion cylinders. The extra cylinder is also referred as exhaust cylinder, since it uses the exhaust gases emanating from the combustion cylinders. This cylinder has no valves and has no combustion inside. Further details and features of the engine concept are described in section 2.5.

The transport industry has been witnessing an increase in the stringency of emission norms which requires effective emission reduction technologies across the product portfolio. Furthermore, it is incumbent on vehicle manufacturers and Original Equipment Manufacturers

(OEMs) to meet customer demands within the aspects of fuel efficiency and performance. Turbocharging has been a fruitful technology strategy for achieving these objectives for both non-hybrid and hybrid engines over a long period of time. However, there are various sub-strategies existing under turbocharging depending upon the application and operating characteristics of the vehicle segment [35].

Turbocharging in general, also comes with certain downsides. These limitations have been explained in detail in sub-section 2.3.3. It points out that there is a trade-off between the best operating regions in small and large-sized turbochargers. At the low Revolutions Per Minute (RPM), smaller turbos are more efficient compared to larger turbos. On the other hand, large turbos are more efficient at the higher RPM. Electrically-assisted turbos and VGTs are strategies used under turbocharging to combat the above problem. However, some problems related to electrically-assisted turbochargers are system complexity and extra energy requirement in the battery pack [27]. VGTs are promising when it comes to tackling the aforementioned challenge but are more sensitive to higher exhaust temperatures [7] [27]. It has been pointed out that the variable nozzles are sensitive to higher temperatures, thus affecting reliability and endurance negatively [7]. With the need for hybridization of powertrains, manufacturers are also keeping an eye on turbocharged engines with fewer cylinders. In the patent [27], it has been pointed out that engines with fewer cylinders have uneven exhaust. This means that the exhaust pressure has high variation with time and thus has a less ability to provide high continuous exhaust pressure to the turbocharger inlet, when compared to engines with more cylinders. Twin-scroll turbochargers are typically deployed to combat this issue by reducing the pressure interference between the cylinders. In such a technical solution, two separate exhaust manifolds are used to drive the exhaust gases to the turbine inlet. Thus, higher pressure waves enter the turbocharger across the engine cycle. From the cost of manufacturing perspective, it is relatively more expensive to produce and package compared to single-scroll turbochargers, due to its higher machining complexity [36].

The EPTE concept earlier mentioned in this sub-section has been conceived and formulated with the intention to provide a technical solution to the aforementioned challenges with respect to turbocharging, and to also offer higher expansion ratio relative to compression ratio, with a solution that does not add complexity and pumping losses. To bring such solutions into the market, it is vital for any manufacturer to gain an overall sense of the system performance before building prototypes and hardware components. This requires product development based on simulation approaches to predict the holistic impact of the system in environments which would replicate the operating conditions. This forms the core foundation of the thesis work.

1.2 Purpose

The purpose of this thesis work is to realize the technical potential of the EPTE concept. The assessment process of technical potential is based on analyzing the turbocharged ICE performance and some critical gas exchange parameters in the exhaust side using a commercial engine simulation software, GT-Power^{TM}. This software is developed and sold by Gamma Technologies. The technical potential of the EPTE concept is measured against a turbocharged baseline engine, which does not have the exhaust cylinder component. All other components and geometrical aspects of the baseline engine are the same as the EPTE concept.

In the context of the thesis work, performance analysis refers to assessment of Brake Specific Fuel Consumption (BSFC) and Brake Power (BP) of both the engines, whereas the gas exchange parameters refer to the pressure variation before and after the turbine component. A side objective was to analyze the percentage of total BP contributed by the exhaust cylinder component in the EPTE concept.

Serving the above purpose will help the relevant stakeholders to have a system-level view of the engine concept before beginning any prototype building activity during the pre-development process. The relevant stakeholders have been highlighted in sub-section 1.4.

1.3 Research Questions

Before beginning the thesis work, a literature study was performed connected to the assessment study. This part is discussed in detail in Chapter 2. Based on the literature analysis, research questions were formulated to devise the project roadmap. The research questions ultimately relate to the overall purpose of the thesis work. These are framed below:

1. What is the EPTE concept and what theoretical benefits does it provide compared to the conventional turbocharged ICE topology? Note that conventional turbocharged ICE represents the topology without the extra cylinder component.

2. How should the sizing and modelling of the exhaust cylinder be performed in a commercial engine simulation software and what input conditions does it require?

3. By what percentage is the EPTE better than the conventional turbocharged ICE topology within the aspects of BSFC and BP, at different intake boost pressure limits?

4. What percentage of the total brake power produced at the crankshaft is contributed by the exhaust cylinder in the EPTE?

5. How does the crank-resolved exhaust pressure vary for both the engines, before and after the turbine?

6. What are the hardware modifications in the intake and exhaust side required for the EPTE model to produce the benefits from the performance metrics standpoint, when compared to the baseline engine?

7. What impact do the baseline engine and EPTE models have on the flywheel weight and sizing?

1.4 Stakeholders

The stakeholders related to this thesis work are envisioned as the individuals and relevant groups who have interest in the outcome of the thesis project. These individuals and groups are directly or indirectly affected by the findings of this work. In this context, the relevant stakeholders are listed as follows:

1. *Internal stakeholder* : Mats Olshammar, the inventor behind the patented concept [27] and his company Olshammar Nebula AB which is the owner of the patent.

2. *External stakeholders* : OEMs and vehicle manufacturers, which can develop, adopt and commercialize the engine concept. OEMs could be suppliers of holistic engine systems or producers of engine hardware components like turbochargers etc.

1.5 Limitations and Delimitations

This section includes the limitations and delimitations related to the thesis project. Limitations are influences that the researcher or the thesis worker does not have control over. On the other hand, delimitations refer to the choices made by the researcher in a project. Delimitations represent the boundaries of any scientific or engineering work performed. The delimitations were decided based on a mutual agreement between the thesis workers and the internal stakeholder involved. This decision was based on the purpose and the goals of the assessment study.

1.5.1 Limitations

1. The simulation-based assessment is bounded by the software limitations of GT-Power^{TM}. GT-Power ^{TM} is a simulation tool widely used in the transport industry for predicting performance of complete engine systems. It is a one-dimensional flow solver which accounts for the flow, heat transfer and friction effects in the engine [38]. The flow parameters are considered as uniform in the cross-section of the components, whereas realistically the flow field is non-uniform in the cross-sections.

2. The software allows only one crankshaft component in an engine model. This limitation leads to a delimitation which is described in sub-section 1.5.2.

1.5.2 Delimitations

1. Due to the software limitation of allowing not more than one crankshaft in the engine model, the thesis work was restricted to the (2+1) setup ideated in the patent [27]. The patent also advocates different topologies such as the (3+1) and the (4+1) setup, which require two separate crankshafts, one for the firing combustion cylinders and other one for the exhaust cylinder . The (2+1) setup represents two combustion cylinders and one exhaust cylinder. The same representation applies for both the (3+1) and (4+1) setup.

2. The assessment study in the thesis scope does not include the comparison of the baseline engine and the EPTE from the exhaust emissions standpoint, as it does not form a part of the core purpose as per section 1.2.

3. Knocking phenomena was not investigated in the assessment study, as it does not form a part of the core purpose.

4. The engine models were simulated in steady-state conditions for having a reasonable balance between internal validity and computational power.

5. The baseline engine and EPTE models were modelled as Spark-Ignition (SI) engines running on gasoline fuel.

6. For turbocharger modelling, *TurbineSimple* and *CompressorSimple* models were used from the software library, for both the baseline engine and EPTE concept. These models are generally used in the absence of turbocharger maps from manufacturers, and when new charging concepts or turbocharger matching is required for an engine. There were no turbocharger maps available from any manufacturer

during the thesis work, which motivates for such a choice. However, such a modelling simplification also provides a detailed analysis of the gas exchange system and its interaction with the engine combustion system. More specific details of the *TurbineSimple* and *CompressorSimple* models have been described in chapter 3.

7. The analysis conducted was purely based on the results emanating from the simulation study. Therefore, it does not encapsulate results from experiments or prototype testing. However, the main purpose of the thesis work was to gain an overall sense of the performance of EPTE using a commercial engine simulation tool, before commencing hardware development activities for the concept.

1.6 Research Approach

This section gives a brief description of the research methodology adopted for the thesis work. It summarizes the approach used for creating the EPTE model in GT-Power^{TM}. In addition to this, it also gives an overview of the simulation-based concept assessment study procedure. Figure 1 shows the process by which the EPTE model was devised in the software. Figure 2 depicts the methodology overview related to the thesis work.

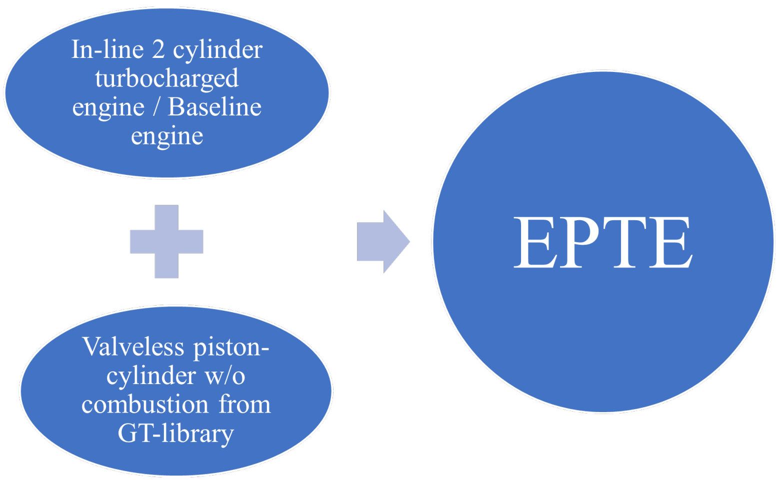

Figure 1: EPTE model creation in GT-Power^{TM}

A pre-existing in-line 4-cylinder naturally aspirated SI engine model was imported from the examples library in GT-Power^{TM}. This naturally aspirated 4-cylinder engine was converted to a 2-cylinder engine by removing 2 cylinders and the relevant pipe connections attached to it. The 2-cylinder engine was then integrated with a turbocharger using *TurbineSimple* and *CompressorSimple* models from the template library. Finally, this represented the baseline engine model. Figure 1 shows that the EPTE model was created by adding an exhaust cylinder component to the baseline engine. In the context of GT-Power™, the exhaust cylinder component is called as *Piston-Cylinder w/o combustion*. This component is available in the template library and it acts as a reciprocating compressor-expander. It should be noted that the exhaust cylinder incorporated in the EPTE model does not have any inlet or outlet valves. More specific details of the exhaust cylinder component used in the engine model are explained in chapter 3.

After both the engine models were created, some DOE studies were run to gain insights into a common range of engine variables which gave sweet spot for the engine models from a BSFC and BP standpoint. The engine variables under consideration were some critical intake and exhaust parameters. This range for different engine variables were then used for optimizing both the engine models in the Integrated Design Optimizer (IDO), a dedicated optimization tool within GT-Power™. The optimized engine models were then used for comparison of performance and gas exchange parameters. This whole process is depicted in figure 2. More specific details about the engine variables and the optimization approach are explained in chapter 3.

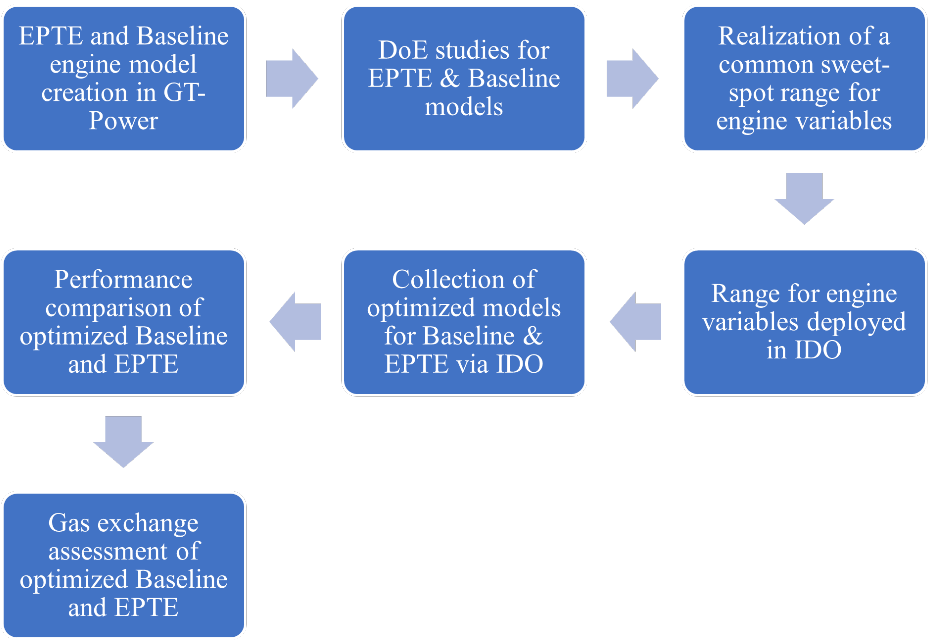

Figure 2: Overview of thesis method

1.7 Outline

This section describes the content of individual chapters related to the thesis report.

- In chapter 1, the background information of the thesis is described to provide an overall sense of the project scope and purpose.
- In chapter 2, a systematic literature review as a frame-of-reference is conducted. This particular chapter provides a general view of turbocharging in ICE, its drawbacks and currently available sub-technologies under turbocharging in the market. Information regarding over-expanded cycles is provided before the EPTE concept is explained in detail.
- In chapter 3, the method and implementation approach incorporated across the simulation-based assessment is explained. It discusses some prominent features of the software GT-Power^{TM}, which are most critical to the modelling of baseline engine and EPTE.
- In chapter 4, the results are analyzed, comparing the performance and gas exchange metrics of both the engines models.
- In chapter 5, the results are consolidated in such a way that it provides a systematic picture to the reader on how the answers to the research questions were delivered. It also provides some recommendations which would foster the development process of the EPTE concept.

Chapter 2

Frame-of-Reference

In this chapter, a systematic review is provided of the literature, which helped to perform the thesis work holistically. It covers all relevant engineering aspects pertaining to the concept and provides a theoretical foundation on which the rest of the tasks were performed.

2.1 Four-stroke cycle

The ICEs under consideration in this thesis are spark-ignition (SI) engines (sometimes called Otto engines, or gasoline or petrol engines, though other fuels can be used). A French patent filed in 1862 to Alphonse Beau de Rochas outlined the fundamentals of four-stroke cycle [17]. Reciprocating engines are those where pistons travel back and forth in the cylinder. It transmits power from high pressure and high temperature burnt gases within the cylinder to a drive shaft via the piston, connecting rod, and crank mechanism. The four-stroke cycle is widely employed in reciprocating engines. To complete one cycle of operation, each cylinder takes four piston strokes (2 crankshaft rotations) [16]. Four strokes are as shown in figure 3.

1. *Intake stroke*: It begins at Top-Dead-Center (TDC) and ends at Bottom-Dead-Center (BDC), pulling new air or a fuel-air combination into the cylinder. The intake valve opens just before the stroke begins and closes just after it stops to enhance the mass introduced [16].

2. *Compression Stroke*: When the piston is at BDC, the compression stroke begins and finishes at TDC, when the air-fuel mixture is compressed to a small fraction of its original volume. Combustion begins at the end of the compression stroke, and the cylinder pressure rises rapidly [16].

3. *Power stroke*: As the high-temperature, high-pressure gases push the piston down and cause the crank to rotate, the expansion stroke begins at TDC and finishes at BDC. During the power stroke, the piston has to do about five times as much work as it did during compression. The exhaust valve opens when the piston approaches BDC, enabling the exhaust process to begin and reducing the cylinder pressure to equal the exhaust system pressure [16].

4. *Exhaust stroke*: The piston moves from BDC to TDC. The leftover burnt gases escape the cylinder in two ways: first, since the cylinder pressure may be substantially higher than the exhaust pressure; and second, when the piston advances toward TDC, these gases are pushed out by the piston. The inlet valve opens as the piston approaches TDC, and the exhaust valve closes immediately after TDC. The cycle then repeats itself [16]. The intake and exhaust valves can be kept opened at the same time (referred to as valve overlap) so that fresh air can flush out the remaining exhaust gases.

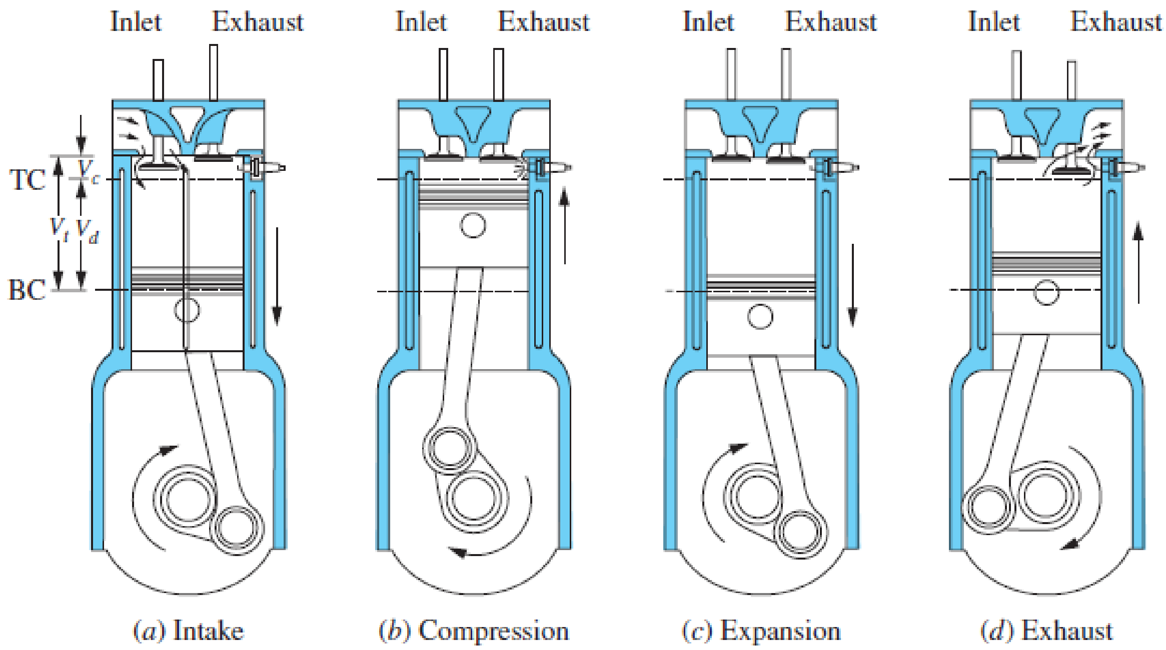

Figure 3: Four-stroke operating cycle [16]

2.2 Engine Flywheel and Torque Fluctuations

A flywheel is an energy storage device which absorbs and stores energy when the supply is more than the requirement. It then releases the stored energy when the energy required exceeds the supply [29]. In the context of an ICE, energy is produced during the power stroke but it runs throughout the engine cycle covering all strokes. This is achieved with the help of a flywheel. Apart from this functionality, flywheels are also used for providing ring gear attachment for starter motors and facilitating the integration of the transmission via clutch.

Two important aspects related to an ICE operation are the instantaneous angular velocity and torque. These parameters directly affect the combustion efficiency, power and vibrations of the combustion engine [34]. The torque and the angular velocity are intermittent across the whole engine cycle. The gas pressure inside the combustion cylinders fluctuates throughout the cycle, thereby contributing to torque fluctuation. The acceleration and deceleration of the piston assembly contributes to the fluctuation in angular velocity [29] [34]. These combined fluctuations lead to a fluctuation in the turning moment produced at the crankshaft. Adding more combustion cylinders in such a system can help tackling such an issue only to a certain extent. Therefore, flywheels are necessary to offset this challenge of fluctuating torque levels across the whole engine cycle. Having such a component helps the engine to produce a relatively smoother torque across the whole engine cycle. According to engine theory [29], the inertia of the flywheel attached to the crankshaft is directly proportional to the fluctuation in torque. Therefore, an ICE with higher torque fluctuation would need a relatively heavier and larger flywheel i.e. with higher moment of inertia.

2.3 Engine Downsizing and Turbocharging

Automobile powertrains must become more efficient in order to meet stricter emission and fuel economy regulations. To meet the requirements, manufacturers are converting naturally aspirated engines into boosted engines with smaller displacements. This method is referred to as ‘engine downsizing’. The average engine load is higher, and an increased average efficiency is achieved by substituting with a smaller engine. When a combustion engine is subjected to high loads, its efficiency is at its peak [19]. The use of forced induction compensates for the lower power output caused by the smaller engine displacement. The most common type of forced induction system is the turbocharger system. It comprises of a compressor and a turbine linked by a single shaft. The turbine recovers the engine’s leftover exhaust energy, which is then used to power the compressor [24]. In gasoline engines, turbocharging and downsizing have led to substantial fuel economy improvements, close to a 20% reduction [33]. The engine's increased breathing capacity is the main reason. Harnessing waste exhaust energy to increase the intake charge density flowing into the engine is a sustainable strategy. Figure 4 depicts a basic turbocharger with wastegate and intercooler. The boost pressure of the inlet air after the intercooler is referred to as p_{boost}, and the pressure of the inlet air in the intake manifold is referred to as p_{man}.

2.3.1 Wastegate

Overspeeding the turbocharger and gaining too high boost levels and cylinder pressures frequently demands bypassing some of the exhaust around the turbine. A wastegate or bypass valve is integrated in the turbocharger casing. It comprises of a spring-loaded valve that responds to the pressure acting on a regulating diaphragm from the intake manifold. The sum of the turbine mass flow rate and the wastegate mass flow rate equals the total engine exhaust mass flow rate. Only a portion of the exhaust gases go through the turbine and produce power while the wastegate is open; the remainder flows directly into the exhaust system downstream of the turbine [18].

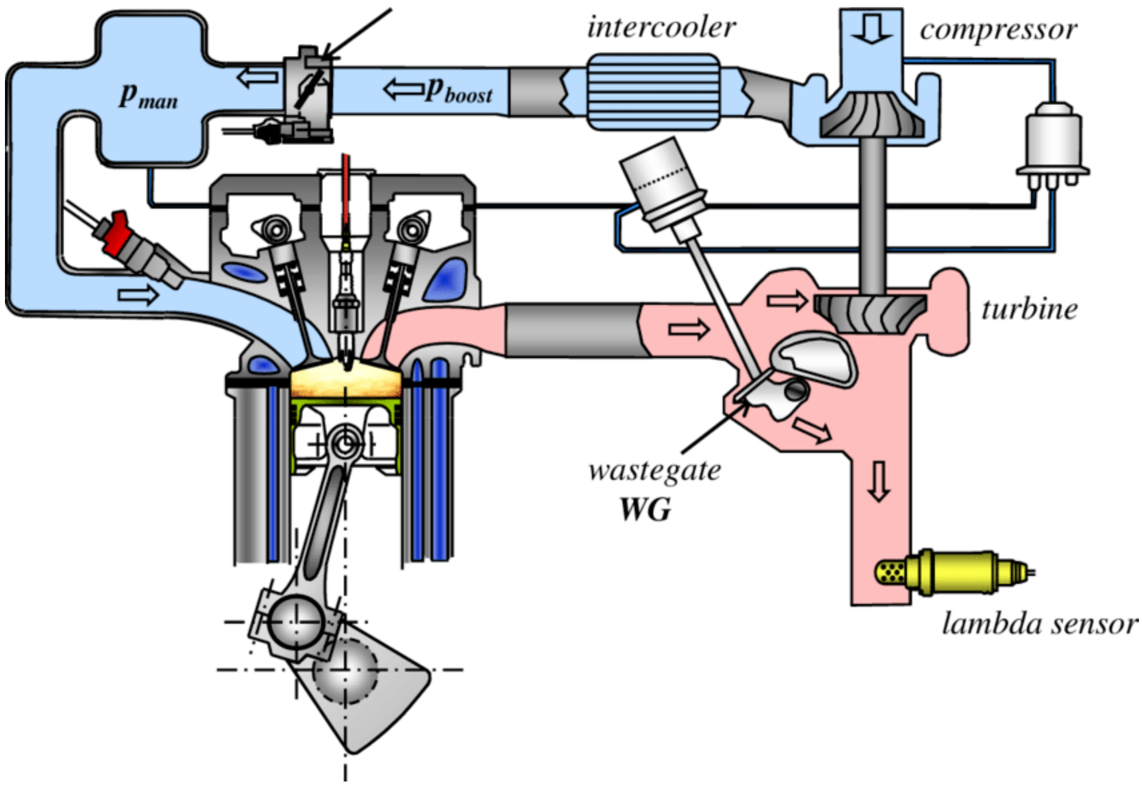

Figure 4: Turbocharged engine setup [4]

2.3.2 Intercooler

After compression, just before gas enters the cylinder, charge cooling with a heat exchanger (also referred as an intercooler) is widely used to lower the temperature of the air. Consequently the inlet air density increases. Typically, an intercooler is installed between the compressor and the engine's intake manifold. By lowering the temperature of the air coming out of the compressor outlet, in-cylinder knocking can be reduced [18].

2.3.3 Problems related to turbocharging

Apart from enhancing the volumetric efficiency of an ICE, turbocharging presents a number of challenges. For starters, there is a compromise between ideal operating zones with small and big turbochargers.

Small turbochargers, for example, perform better at low engine speeds than high engine speeds. Small turbos may spool up faster at low engine RPM, due to the decreased inertia of the turbine and higher pressure in the smaller orifice. Because of the faster spooling, the turbocharger may reach a suitable boost pressure ratio at low engine RPM. At high engine RPM, the massive quantity of exhaust gas might cause mechanical failure in the smaller turbine wheel and compressor choking. High exhaust mass flow into a smaller turbine could also lead to high engine back-pressures. High back-pressures can lead to more pumping losses and thereby further efficiency reduction [36].

On the other hand, big turbos have promising efficiencies at high engine RPM but not at low RPM [27]. This is because at low RPM, the exhaust flow pressure is not sufficient to provide enough boost to start spinning the turbocharger. The minimum engine speed required for the turbocharger to spool up is called the boost threshold. For this reason, it is vital to match a suitable turbocharger with the engine.

The exhaust flow from the cylinder is not uniform and exhaust gas pressure peaks are formed (p_{eg}) which is indicated by figure 5 in the following page. Pressure wave travels through the exhaust manifold causing a pressure drop after p_{eg}. This pressure can drop below the turbine inlet pressure (p_t) [36].

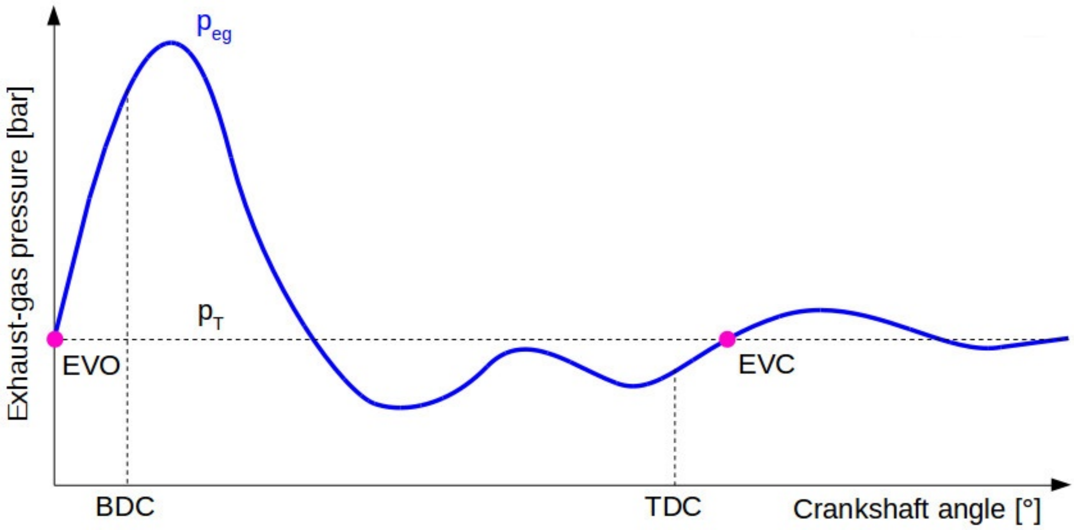

Figure 5: Exhaust gas pressure wave [36]

The exhaust process in the ICE is characterized by 3 phases [36]:

1. Blowdown phase (period between exhaust valve opening and TDC)
2. Backward displacement stroke
3. The scavenging phase (valve overlap)

2.4 Current Concepts and Technologies

In this section, commercial technological solutions currently available related to turbocharging and over-expanded cycle-based concepts have been discussed from a holistic standpoint, which form a foundation for the EPTE concept. This is because the EPTE concept is claimed to increase the efficiency of the turbocharger and contribute to the over-expansion of gas due to the presence of an EXC [27].

2.4.1 Twin-scroll turbochargers

Single and twin-scroll turbochargers are generally two approaches towards turbocharging strategy. 'Scroll' refers to the turbine housing (or turbine manifold, or volute) that connects between exhaust manifold and the turbine rotor.

Single-scroll turbochargers use a common exhaust manifold for all cylinders, as stated by [36]. Each cylinder's exhaust ports are linked to a collector, which is a shared volume. As a result, before reaching the turbine, the exhaust gas pressure waves from each cylinder interact and reduce the pressure peaks. This technique guarantees a steady pressure continuous flow to the turbine rotor, but the pressure dampening results in a loss of usable exhaust gas energy [28]. The single-scroll turbocharger provides cost effective, easy to produce and good performance at increased exhaust gas flow. But it suffers in performance at low to medium RPM and engine loads [36]. The back pressure increases in multi-cylinder engines resulting in low scavenging and consequently, diluting the intake charge which affects engine performance.

By integrating different exhaust manifolds from the cylinder exhaust ports, the twin-scroll turbocharger approach helps to prevent this issue. This system features a split turbine housing and a well designed exhaust manifold that couples the appropriate cylinders to direct exhaust gases into each scroll separately [8]. The turbine housing (or volute) is divided meridionally into two scrolls and each inlet feeds the entire turbine rotor circumference. This design saves energy from exhaust gas and improves cylinder gas exchange [30]. The firing order of a four-cylinder engine is usually 1-3-4-2. The exhaust channels from the two pairs of cylinders are linked to the turbine via separate scrolls of various diameters, as shown in figure 6 and explained by [36]. The wider channel A, which connects cylinders 2 and 3, guides one exhaust stream to the turbine blades' outer edge, allowing the turbocharger to spin quicker. The narrower channel B connecting cylinder 1 and 4 guides the other exhaust stream onto the inner surfaces of the turbine blades and therefore improves the turbocharger responsiveness during the engine's transient operation.

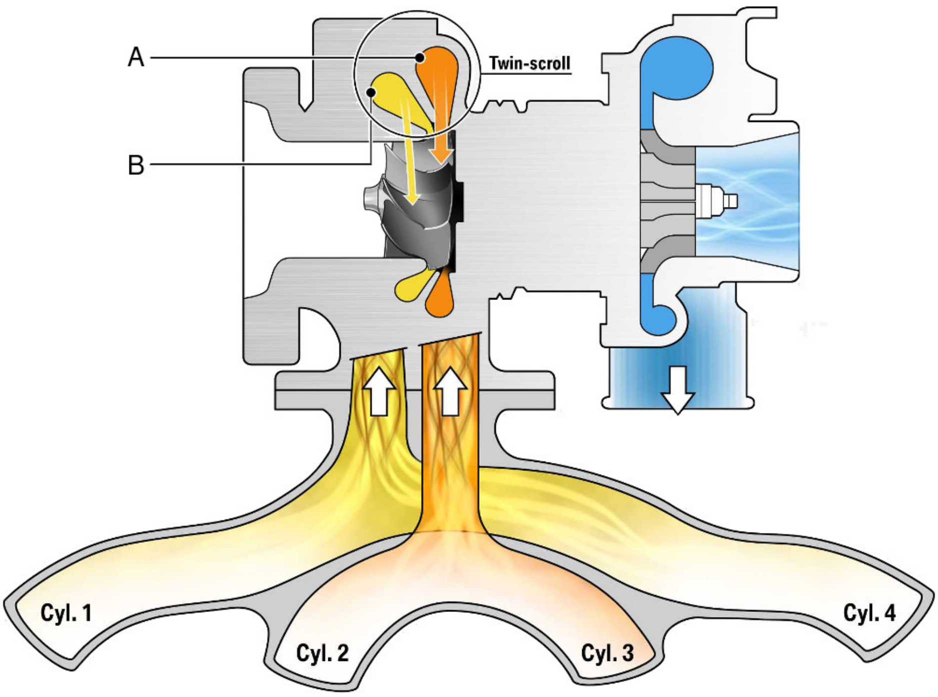

Figure 6: Twin-scroll turbocharger in a 4-cylinder engine [36]

This configuration of twin-scroll turbocharger offers excellent low-end torque as well as better high-end power. Along with this, it also offers better engine scavenging due to reduced back pressure and non-interaction of exhaust pulses, reduced engine pumping loss, increased turbine efficiency and lower fuel consumption [8]. But twin-scroll turbochargers are more complex in design due to smaller exhaust runners compared to a single-scroll turbocharger. This complexity leads to higher manufacturing costs of the exhaust manifold and turbine casing for a twin-scroll turbocharger [36]. During unequal admission (different exhaust mass flow rate in the two turbine scrolls) or partial admission (exhaust mass flow in only one scroll), efficiency of the turbocharger can be reduced due to cross flow between the two turbine scrolls, especially if the turbine has unequal volute geometries [37]. Due to additional exhaust manifolds, the system will also require additional wastegate and dumptube which results in a bulkier turbocharger, which creates a negative effect to engine compactness.

2.4.2 Variable Geometry Turbochargers (VGTs)

VGTs have emerged as a potential commercial option as the demand increases for optimal turbocharger efficiency throughout the operating range. A variable nozzle area control mechanism is included in this system, which aids in maintaining adequate levels of turbocharging efficiency at all RPM [7]. Figure 7 depicts a cross-sectional view of the technology and the operating mechanism at low and high engine speeds.

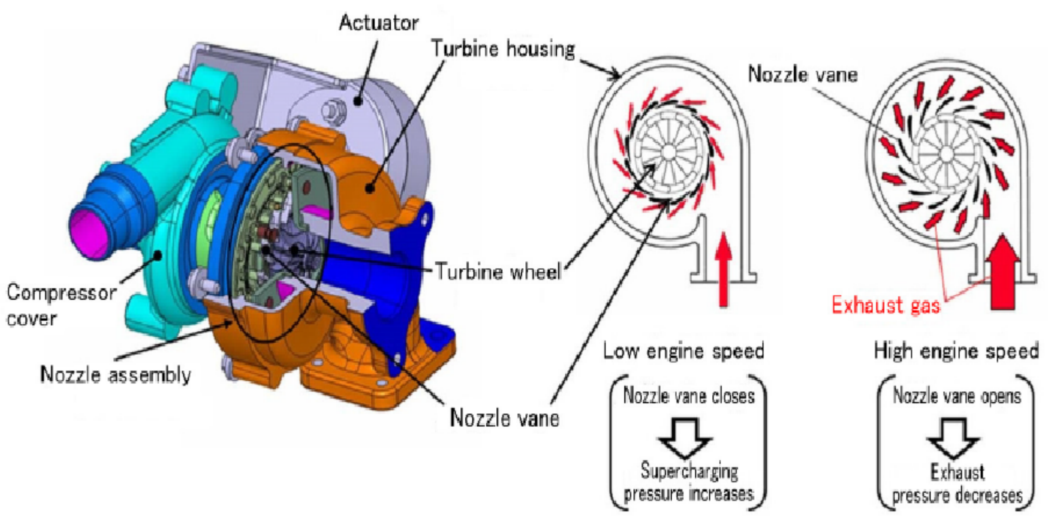

Figure 7: Cross-sectional view and functions of VGT [7]

A correctly tuned engine with variable nozzle guarantees that the exhaust-pressure increases at low RPM and drops at higher RPM, as described in figure 7. The closing and opening of the nozzle is assisted by an actuator. However, Ebisu et al. [7] highlighted certain technological problems with VGTs, based on a technical report by Mitsubishi Heavy Industries. Regulating the variable nozzle geometry is difficult because fluctuating exhaust pressure can cause pre-ignition and knocking issues within the combustion cylinder. This is especially problematic in gasoline engines, as higher boost pressure can cause hotspots inside the cylinder [7]. In addition, gasoline engines produce greater exhaust temperatures than diesel engines. This raises the expense of developing a variable nozzle turbine for gasoline engines since high-temperature resistant materials are required. An Exhaust Gas Recirculation (EGR) would counter this issue, but the complexity of the system increases.

2.4.3 Electrically-Assisted Turbocharger (EAT)

The only power source for the turbochargers are the exhaust gases. This topology is subject to poor mechanical responsiveness and low efficiency. This is typical when the engine speed is low, as noted by Bumby et al. [2]. This holds true even with the addition of the twin-scroll turbochargers and VGTs described in subsections 2.4.1 and 2.4.2. The electrification of turbochargers is a solution to the above. This system is also known as the Electric Forced Induction System (EFIS). Some advantages of EFIS over non-electrified systems are:

- higher transient response (reduced turbo lag),
- increased engine output power,
- energy regenerative capability,
- applicable to fuel cell vehicles [22].

There are different EFIS topologies, but the topology of interest is the EAT. This topology is shown in figure 8.

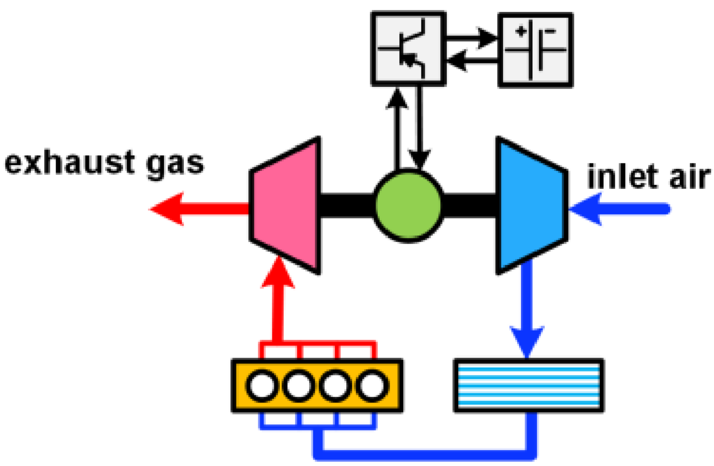

Figure 8: Schematic diagram of EAT [2]

According to Bumby et al. [2], a high-speed electric machine is linked between the turbine and the compressor. At low RPM, the electric machine acts as a motor, giving more torque to the compressor. This results in higher boost pressure and faster transient response. The electric machine creates power at higher RPM, which may be stored in a battery. It can also limit the turbine speed. But this may result in a significant back pressure in the engine, cancelling the energy recovered from exhaust gases [2, 5].

Bumby et al. [2] also highlighted the advantages and disadvantages of EAT. Improved boosting at low RPM, self-sensing capability of the electric machine rotor position, motoring and generating capabilities, and the requirement of electric components with lower power output, which implies cheaper cost, are all benefits of this topology [21]. Reducing the high-temperature effect on the electric machine when the machine is located within the turbocharger is a difficulty with this topology. Switched reluctance machines, Induction machines or flux-switching permanent magnet machines can be utilized for this topology since they are more suitable for high-temperature operation and thermal management than surface permanent magnet machines. However, significant switching losses, poor heat dissipation, and electromagnetic interference hamper these high-speed electric devices. Mechanical losses in the form of stress on high-speed electric machine components, particularly the rotor and ball bearings, may also occur [2]. As indicated in section 1.1, EAT also requires an extra battery as well as additional electrical components.

2.4.4 Miller cycle

The major disadvantage of engine downsizing, as stated by Nhut [24], is the large percentage of wasted exhaust gas energy which cannot be efficiently recovered. This percentage can be minimized by using over-expanded cycles. An overexpanded cycle is a cycle where the effective expansion ratio exceeds the compression ratio. Ralph Miller [23] proposes that varying Inlet Valve Closing (IVC) timing is a simple approach to accomplish over-expansion in standard crank mechanism engines. According to [20], overexpanded cycles are also known as Miller or Atkinson cycles, after their inventors, Ralph Miller and James Atkinson respectively. The literature is not uniform in the use of these terminologies. According to Environmental Protection Agency (EPA) [6, 20], the Atkinson cycle is an over-expanded cycle with Early Inlet Valve Closing (EIVC) or Late Inlet Valve Closing (LIVC) in engines that does not feature any forced induction systems, whereas the Miller cycle is an Atkinson cycle boosted by either a turbocharger or supercharger. According to Schutting et al. [32], the over-expansion achieved via Variable Valve Timing (VVT) of the intake valve is credited to Ralph Miller (called as

Miller cycle), whereas James Atkinson should be credited with the over-expansion achieved by modifications to the cranktrain mechanism (called as Atkinson cycle). The difference arose due to Miller's proposed cycle, which solely considered EIVC while David Luria achieved the Atkinson cycle and named it the Otto-Atkinson process by incorporating LIVC instead of a complex crank mechanism [38].

Modern practices use either EIVC or LIVC to achieve over-expanded cycles. Jääskeläinen [20] further explains that, at the end of the compression stroke, EIVC and LIVC predominantly lowers the in-cylinder temperature. This allows for increased geometric ratios that in turn provide a higher expansion ratio resulting in improved efficiency. The geometric compression ratio is increased by increasing the expansion ratio while keeping the effective compression ratio close to the base value. The consequence would be a reduction in Brake Mean Effective Pressure (BMEP), as indicated by Branyon and Simpson [1], but an increase in thermal efficiency. Typically, the Miller cycle is used in conjunction with turbochargers. The loss in BMEP can be recovered with a higher intake boost pressure limit. Because of the shorter compression stroke, the Miller cycle essentially has no efficiency benefit as shown by Wu, Puzinauskas, and Tsai [39]. Therefore, the Miller cycle is beneficial when used with a turbocharger or supercharger. The Otto cycle's pre-ignition or knocking problem, on the other hand, may be mitigated by cooling the air–fuel mixture before combustion by either EIVC or LIVC.

2.4.5 Schmitz five-stroke engine

A majority of ICE in the market work on the four-stroke cycle, which is described in detail in section 2.1. With higher expansion ratios obtained in the power stroke, more work can be extracted out of the system. But in conventional four-stroke cycles, the effective compression ratio is equal to the effective expansion ratio. In 2003, Gerhard Schmitz came up with a concept to decouple the compression and expansion ratios, which allows the engine to have higher effective expansion ratios, and facilitated an increased power density and higher power output of the ICE [31]. This was achieved by adding an extra cylinder where, a second expansion of the exhaust gases occur. This cylinder is a Low-Pressure (LP) cylinder with a larger displacement working on a two-stroke cycle. Due to the additional expansion stroke, this engine concept is referred to as a five-stroke engine. The power density is increased by using a turbocharger to supply compressed air as intake.

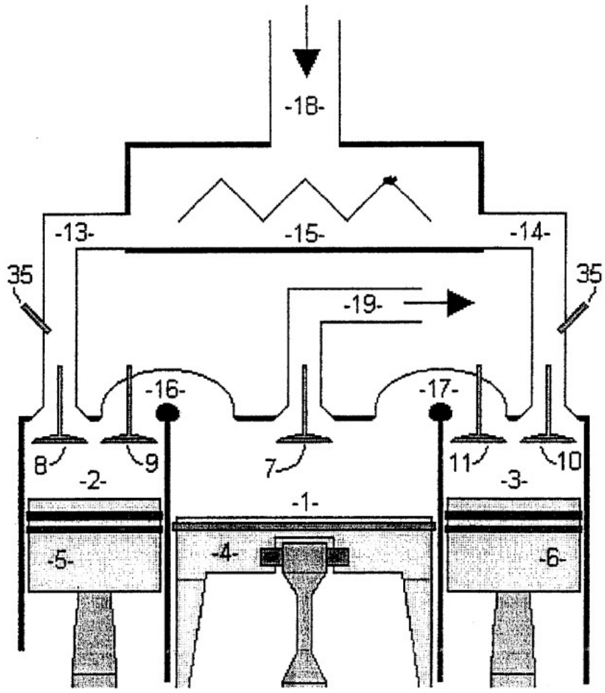

Figure 9: Five-stroke engine setup [31]

General setup of the five-stroke engine is shown in figure 9. The system consists of two High-Pressure (HP) firing cylinders, a LP cylinder with no firing and a turbocharger setup (after part 19). The HP cylinders perform the intake stroke, compression stroke and the first expansion stroke (or power stroke). The compression and expansion ratios are equal till this point. The gases of combustion from the two HP cylinders later move to the LP cylinder via part 16 & 17 where a second expansion stroke occurs before sending the gases into the exhaust manifold (part 19). This increases the effective expansion ratio, which is now calculated as the product of volume ratios of the two expansion processes [31]. The thermodynamic efficiency is increased due to more work being extracted from each five-stroke cycle. The overall compression ratio remains unchanged during the cycle at nearly 7.0:1 while the effective expansion ratio is 14.5:1. The concept can also be extended to a 5-cylinder configuration with three HP cylinders and two LP cylinders. This concept was developed by Ilmor Engineering which built a working prototype. Apart from the benefits mentioned above, this concept has additional advantages like:

- The compression ratio can be varied independently of the expansion ratio in order to address knocking effects without affecting the performance of the engine.
- Engine downsizing leads to reduced pumping work and a more compact setup.
- Use of standardized parts without the need for any additional manufacturing processes.

The engine concept has its limitations which are:

- At low loads of operation, the indicated power of this cylinder could be negative or close to zero after considering the cylinder losses. This will negatively affect the engine, due to additional work required to operate the LP cylinder, overcome the friction losses, instead of getting useful work out of it [26].
- According to Olshammar [27], this concept focuses on increasing the fuel efficiency by having higher expansion than compression, but the exhaust valve on the exhaust cylinder prevents direct flow to the turbine. This is negative for the turbine, it increases pumping losses and requires a larger exhaust piston with more friction, when compared to the EPTE concept.

2.5 EPTE Concept

In this section, the invention of a new engine concept introduced in section 1.1 will be explained in detail. This invention concerns an ICE with standard cylinders operating on four-stroke cycle, a turbocharger arrangement and an EXC arranged in fluid communication with the combustion cylinders [27]. The motivation behind the invention is to increase the fuel efficiency while also improving the performance of the turbocharger. This concept identifies the problems of conventional turbochargers explained in section 2.3.3 and also examines the limitations of all the concepts mentioned in Section 2.4. Even though VGTs and EAT address the issues with operating under different workloads, turbo-lag and fuel consumption, there are still some challenges regarding cost effectiveness, reliability and control. The inventor Olshammar realised there is still a need for improvements and developed the EPTE concept. Different topologies of the engine has been proposed by Olshammar in his patent. Due to a limitation in GT-Power^{TM} mentioned in subsection 1.5.1, a (2+1) configuration is considered for the purpose of the thesis. Regardless, other configurations proposed by the author will be reviewed in this section.

The configuration that will be analyzed in this thesis is a (2+1) type as seen in figure 10. It consists of two combustion cylinders (2) and (3). The channels from the two cylinders, (14) and (15) respectively, lead the exhaust gases after power stroke into the EXC (1). The EXC has two ports, each connected to channels (14) and (15), but they do not feature any valves. The outlet of (1) is connected to the turbocharger arrangement via exhaust duct (17) which allows for a fluid communication between the turbine and (1).

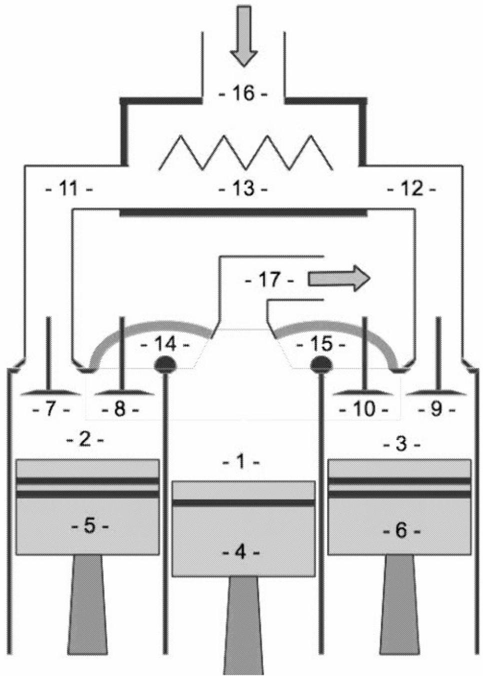

Figure 10: Layout: 2 combustion cylinders + 1 EXC. [27]

The flow of gases to the EXC is controlled by the exhaust valves (8) and (10) provided for (2) and (3). An intercooler (heat exchanger) (13) is provided to cool the intake gas after compression. In the absence of (1), during a complete four-stroke cycle [corresponding to 720 Crank Angle Degrees (CAD)], there will be two exhaust pulses to the turbocharger arrangement, each pulse lasting for 180 CAD, not considering Early Exhaust Valve Closing (EEVC) or Late Exhaust Valve Closing (LEVC) [27]. This pulsating nature of the exhaust gas flow, as seen in figure 11, affects the turbine parts and its performance.

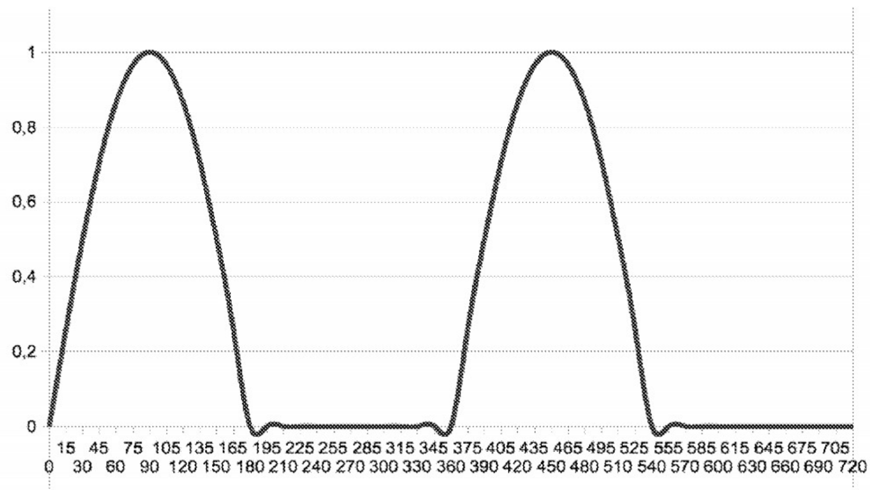

Figure 11: Exhaust pressure waves from a four-stroke engine with 2 combustion cylinders and no EXC [27]

During the exhaust stroke of (2) and in the presence of (1), the exhaust gases exiting (2) are allowed to distribute itself between (1) and (17), such that a portion of the exhaust gases remain in (1) while the remaining exhaust gases drive the turbine. The exhaust piston (4) moves in a direction away from the TDC while the exhaust gases from (2) flows out during the exhaust stroke of (2). By distributing the exhaust gases between (1) and (17), the back pressure is reduced. In the following stroke, when (4) moves towards TDC, the remaining exhaust gases in (1) will be pushed out into (17) and to the turbocharger arrangement.

The exhaust flow in such a case can be visualized in figure 12. The grey line represents the exhaust pressure waves from the combustion cylinders and the black line represents the exhaust pressure waves from the EXC. Hence, the exhaust gases from (2) were distributed over a longer period of time (nearly half the engine cycle) as seen in figure 13. This is beneficial at higher loads, where the otherwise bypassed exhaust gases through a wastegate is instead delayed by the EXC and sent to the turbocharger without any bypass. This increases the turbocharger efficiency [27].

The exhaust duct inlet is arranged in such a way that the exhaust chamber is in fluid communication with the exhaust duct irrespective of the exhaust piston position. By arranging the exhaust duct in the cylinder head, this could be achieved. The engine is allowed for phase shifts between cycles of the first combustion cylinder and the EXC, which will reduce the back pressure and peak pressure of the exhaust at high load situations, and increase the pressure during low load situations. This can be achieved by having the exhaust piston on a separate crankshaft, which is driven by the primary crankshaft. Exhaust piston could also be controlled independently of primary crankshaft with the help of free piston linear generator [27].

With a (3+1) setup, the exhaust piston mounted on a separate crankshaft, rotates 50% faster than the combustion pistons. This is possible due to lesser load on the exhaust piston and the absence of valves in the EXC. This provides a more even mass flow than (2+1) setup. With four combustion cylinders, two configurations are possible, (4+1) or (4+2). A (4+1) setup has four combustion pistons and one exhaust piston that rotates twice as fast as the combustion pistons. in a (4+2) setup, the engine could be 90 degree V4 similar to joining two (2+1) in V-shape. But from the exhaust flow perspective, (3+1) is better among all the configurations, which can be seen in [27].

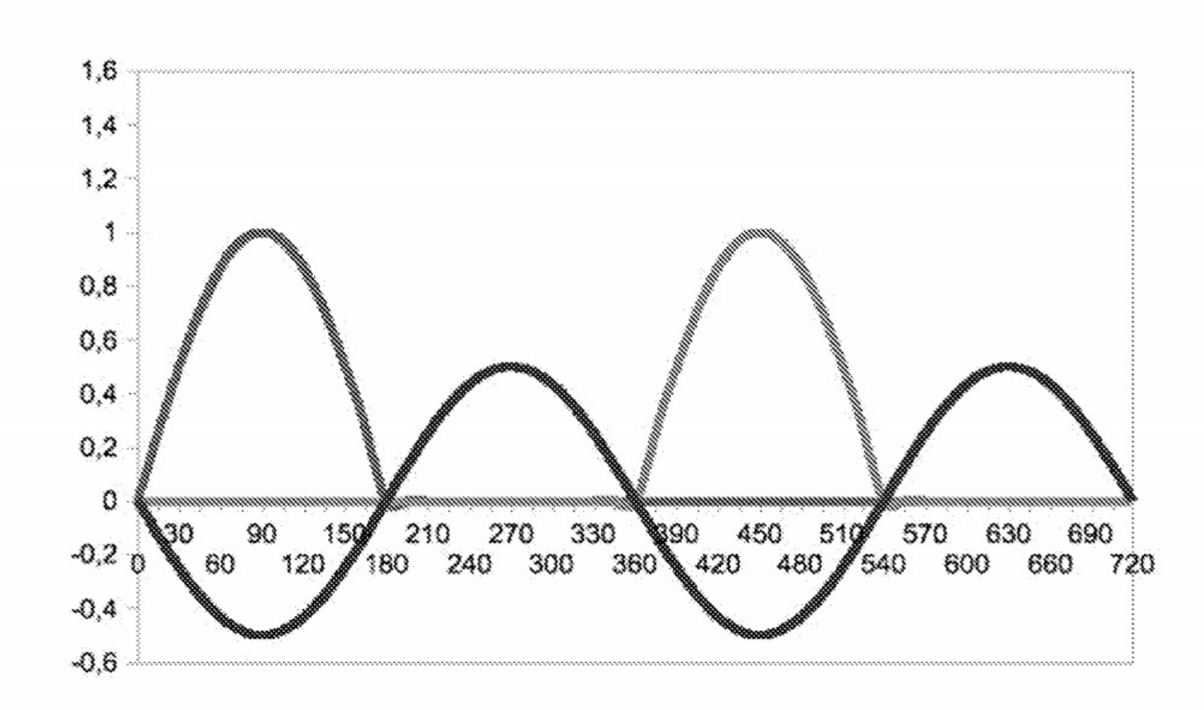

Figure 12: Exhaust pressure waves from a four-stroke engine with 2 combustion cylinders + 1 EXC [27]

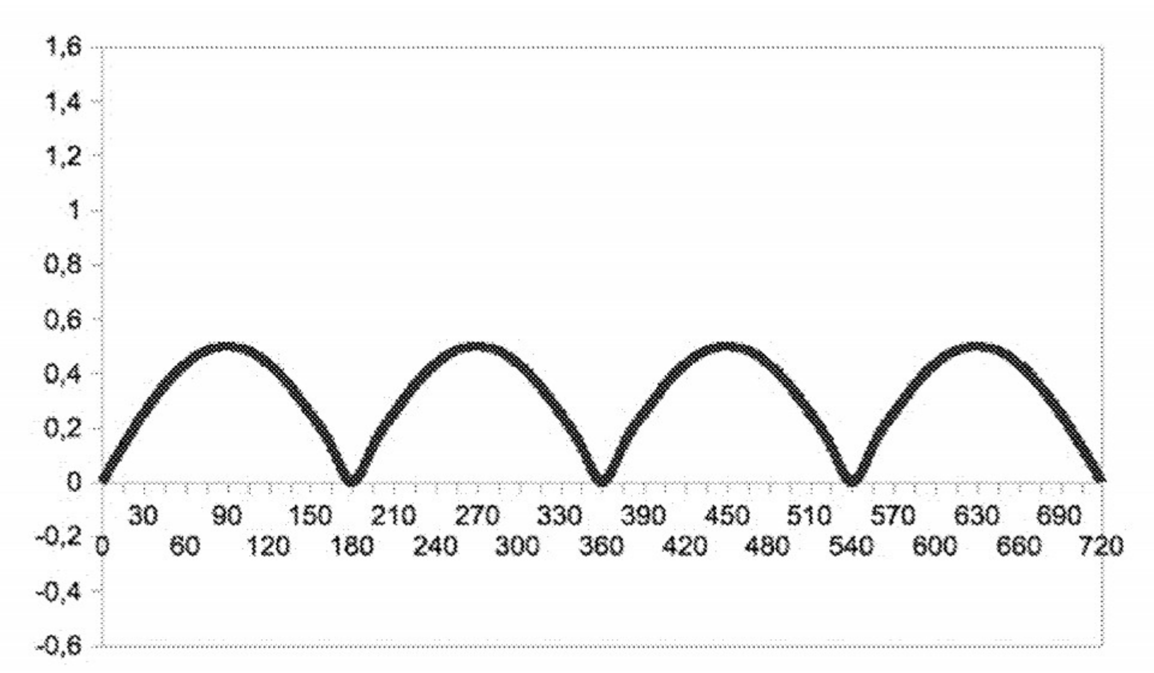

Figure 13: Combined exhaust pressure waves from a four-stroke engine with 2 combustion cylinders + 1 EXC [27]

Chapter 3

Method & Implementation

In this chapter, a detailed explanation about the proposed methodology to conduct studies on EPTE concept is discussed. An overview of requirements specifications from internal stakeholders, modelling theory for engines in GT-Power^{TM}, model generation of the baseline engine and EPTE, model optimization and evaluation process of different performance and gas exchange metrics are described.

3.1 Requirement Specifications

In this section, a compilation of EPTE model requirements are elucidated. Requirements were specified by internal stakeholder which include features, functions and constraints that the models should incorporate. Further, a best suited model was generated, which meets all individual requirements of the concept. These requirement specifications are as follows:

1. The model should be a turbocharged 2-cylinder SI engine. Turbocharger should have a wastegate system that limits boost pressure to a desired value. Engine should also feature an intercooler to cool compressed air by increasing air density at a constant pressure before entering intake manifold. Fuel is injected in the intake port (Port Fuel Injected (PFI)) prior to intake valve, with one injector per combustion cylinder. This model is considered to be the baseline engine model.

2. In addition, the model should have one EXC. Exhaust channels from two combustion cylinders should connect to inlets of EXC, one inlet port for each exhaust channel. Outlet of EXC is connected to turbocharger system via an exhaust duct. Baseline engine model along with the additional EXC constitutes EPTE model.

3. EXC should not feature any valves on either inlet or outlet sides. During an entire cycle of EXC (one expansion stoke and one compression stroke), inlet channels, exhaust chamber and outlet channel should be in fluid communication with each other, irrespective of exhaust piston position.

4. There should be no combustion in EXC. Hence, fuel injection related to this cylinder is zero and there is no firing in this cylinder.

5. During operation, a portion of exhaust gases from either combustion cylinders are expanded in EXC when exhaust piston moves from TDC to BDC. Remaining exhaust gases move directly from inlet to outlet of EXC without being expanded, which will drive the turbine during expansion stroke of EXC.

6. During compression stroke of EXC, expanded gases are compressed into exhaust duct flowing towards the turbocharger.

7. Firing order of engine should be 1-EXC-2. Firing interval between combustion cylinders and EXC should be allowed to vary. Since there is no combustion in EXC, firing, in this case, refers to start of expansion stroke, when exhaust piston starts to move downward from TDC.

8. The models should be built in a way that it allows for a fair comparison between baseline engine and EPTE models. Solver specifications of GT-Power^{TM}, attributes of parts that are not being optimized should be kept constant between both models. Geometry of optimizing parts between the two models should not vary to an extent where a fair comparison between these two models is not viable.

9. Optimization of both models should follow the same approach. Evaluation of these models should be conducted independent of each other in order to eliminate bias and choose the best optimized model in both baseline engine and EPTE.

3.2 Introduction to GT-Power^{TM}

GT-Power^{TM} is a one-dimensional engine simulation software, a product of GT-Suite — a versatile multiphysics platform for creating models of various systems using built-in libraries (flow, thermal, mechanical, chemistry etc.). GT-Power^{TM} is an industry standard software used for designing and developing complete engines. It offers wide range of capabilities with respect to simulating gas exchange process, combustion, heat transfer, in-cylinder motion. More about the features and functions can be found in [15]. The built-in libraries in GT-Power^{TM} offers a multitude of pre-existing engine templates; or different components & subsystems to create custom engine models, along with several controller models for studying the dynamic control of systems.

3.3 Modelling Theory

This section discusses the multiphysics phenomena and different simulation modelling approaches available in GT-Power^{TM}. It also explains relevant theory, governing equations that GT-Power^{TM} employs, useful for understanding the results presented in this report. All equations in this section were derived from GT-Power^{TM} documentation [10, 11].

3.3.1 Flow basics

GT-Power^{TM} utilizes the 1D Navier-Stokes equations to solve the flow models, i.e., the conservation of continuity, energy and momentum equations. All quantities related are calculated as averages across the direction of flow by splitting the whole system into multiple volumes and solving the variables in each volume. Integration of these variables are later done by either an *explicit* time integration method and an *implicit* time integration method. The variables and the range of time step is affected by which integration method the user chooses. More details on how the time step is calculated can be seen in Appendix A.1.

The *explicit* method requires very small time steps, GT-Power^{TM} recommends this method for engine performance studies where unsteady flow and high pressure fluctuations are involved. Mass flow, density and internal energy are the primary variables in the *explicit* method; secondary variables like pressure and temperatures are calculated from them. The governing equations for explicit method are given in Equations 3.1, 3.2 and 3.3, cited from the GT-Power^{TM} documentation [11].

$$Continuity : \frac{dm}{dt} = \sum_{boundaries} \dot{m} \tag{3.1}$$

$$Energy : \frac{d(me)}{dt} = -\rho\frac{dV}{dt} + \sum_{boundaries} (\dot{m}h) - hA_s(T_{fluid} - T_{wall}) \tag{3.2}$$

$$Momentum : \frac{d\dot{m}}{dt} = \frac{dpA + \sum_{boundaries}(\dot{m}u) - 4C_f\frac{\rho u|u|}{2}\frac{dxA}{D} - K_p(\frac{1}{2}pu|u|)A}{dx} \tag{3.3}$$

where, $\dot{m}$ is boundary mass flux into volume ($\dot{m} = \rho A u$), m is mass of the volume, V is the volume, p is the pressure, ρ is the density, A is the cross-sectional flow area, A_s is the heat transfer surface area, e is the total specific internal energy (internal energy plus kinetic energy per unit mass), H is the total specific enthalpy ($H = e + \frac{p}{\rho}$), h is the heat transfer coefficient, T_{fluid} is the fluid temperature, T_{wall} is the wall temperature, u is the velocity at the boundary, C_f is the Fanning friction factor; it will be explained in subsection 3.3.2, K_p is the pressure loss coefficient (due to bend, taper or restriction), D is the equivalent diameter, dx is length of mass element in the flow direction (discretization length) and dp is the pressure differential acting across dx.

Discretization Length

In order to increase accuracy of the model, GT-Power^{TM} splits larger components into smaller segments. This process is called discretization. The software discretizes a pipe into many smaller sub-volumes where each sub-volume calculates the primary variables using Navier-Stokes equations. This discretization length of each sub-volume is smaller than the component length which the user can decide. For engine simulation purposes, GT-Power^{TM} recommends a value for discretization length that offers good balance between accuracy and computation speed. For intake systems, GT-Power^{TM} recommends a discretization length of 0.4 times the bore diameter of combustion cylinder; for exhaust systems, a value of 0.55 times the bore diameter is recommended.

3.3.2 Friction modelling

Friction in components can result in flow losses in the system. In this section, we will see how the losses due to friction are calculated in two major flow components in the model, namely, pipes and engine cranktrain.

Friction losses in pipes

Fluid flow in pipes is affected by friction due to pipe wall and surface roughness. The type of flow, laminar or turbulent, also causes flow losses. The losses are calculated using Fanning friction factor, C_f, which is a function of Reynolds number (Re_D) and wall surface roughness [11]. Two approximations of the Colebrook equation are used to calculate the friction factor. These approximations in GT-Power^{TM} are *'simple'* and *'improved'* methods; they provide faster computational time. GT-Power^{TM} recommends the use of *simple* method for gas circuits and incompressible liquid circuits. *Simple* method is faster and only results in a 5% deviation from the Colebrook equation when used in automotive applications. In the thesis, cast iron (sand roughness = 0.26) was used as the material for all pipe components. It has high surface roughness thus allowing us to model the upper limit of friction losses. The flow regime was considered as turbulent due to pulsations in pressure and flow velocity. The equation for C_f for a smooth pipe (zero surface roughness) in turbulent regime ($Re_D > 4000$), for air and gasoline fluids (both are Newtonian fluids) is seen in Equation 3.4. The value of C_f is later used in the momentum equation.

$$C_f = \frac{0.08}{Re_D^{0.25}} \tag{3.4}$$

Under same conditions, if the surface roughness > 0, then the equation for C_f is given by Nikuradse formula [25], seen in in Equation 3.5.

$$C_{f_{rough}} = \frac{0.25}{\left(2 * \log_{10}\left(\frac{D}{2\varepsilon}\right) + 1.74\right)^2} \tag{3.5}$$

where, ε is the pipe wall sand roughness height and D is the pipe diameter.

Engine friction

GT-Power™ uses several different reference objects to model the mechanical friction of the engine. *'EngineFrictionCF'* is one of them and was used in this thesis [10]. This reference objects can also be used to model auxiliary losses along with engine friction losses. GT-Power™ employs the model by Chen-Flynn [3] in order to determine the engine friction, which is shown below.

$$FMEP = C + (PF * P_{max}) + (MPSF * Speed_{mp}) + (MPSSF * Speed_{mp}^2) \tag{3.6}$$

where, $FMEP$ is the Friction Mean Effective Pressure, P_{max} is the maximum cylinder pressure, $Speed_{mp}$ is the mean piston speed, C is the constant part of FMEP, PF is the peak cylinder pressure factor, $MPSF$ is the Mean Piston Speed Factor and $MPSSF$ is the Mean Piston Speed Squared Factor.

Equation 3.7 states the formula for Friction Mean Effective Pressure (FMEP) in when multiple cylinders are involved. Here, S_i is the instantaneous speed of piston i and $\#Cylinders$ denote number of cylinders in the engine.

$$FMEP_{tot} = \frac{\sum_{i=1}^{\#cylinders}[C + PF(P_{max,i}) + MPSF(\bar{S_i}) + MPSSF(\bar{S_i^2})]}{\#Cylinders} \tag{3.7}$$

$$where,\ \bar{S}_i = \frac{\oint S_i(t)dt}{\oint dt} \tag{3.8}$$

Table 1 shows the values of different friction model attributes used in baseline engine and EPTE simulation models.

Table 1: *EngineFrictionCF* object specifications

ATTRIBUTE	**VALUE**	**UNIT**
Constant part of FMEP	0.4	bar
Peak Cylinder Pressure Factor	0.005	
Mean Piston Speed Factor	0.09	$bar/(m/s)$
Mean Piston Speed Squared Factor	$9e^{-4}$	$bar/(m/s)^2$

3.3.3 Heat transfer modelling

In this section, losses due to heat transfer in pipes and the in-cylinder heat transfer models are described along with relevant equations.

Heat transfer in pipes

Heat transfer occurs between the fluid flowing in the pipes and wall of the pipes. The heat transfer coefficient is used to determine this heat transfer; it is calculated using the Colburn correlation [11]. The Colburn correlation for smooth pipes is given below (Equation 3.9).

$$h_g = \left(\frac{1}{2}\right) C_f \rho U_{eff} C_p Pr^{-2/3} \tag{3.9}$$

where, h_g is the heat transfer coefficient of smooth pipe, C_f is the Fanning friction factor of smooth pipe, ρ is the density, U_{eff} is the effective velocity outside boundary layer, C_p is the specific heat, Pr is the Prandtl number.

Equation 3.10 represents the heat transfer coefficient in pipes with non-zero wall surface roughness. Here, $h_{g,rough}$ is the heat transfer coefficient for rough pipes and $C_{f,rough}$ is the Fanning friction factor for rough pipes [11].

$$h_{g,rough} = h_g \left(\frac{C_{f,rough}}{C_f}\right)^n where,\ n = 0.68 * Pr^{0.215} \tag{3.10}$$

In-cylinder heat transfer

GT-Power™ defines an object called *'EngCylinder'* to model the combustion cylinders in the system. *EngCylinder* combines two sub-objects called *'EngCylHeatTr'* and *'EngCylTWall'*. *EngCylHeatTr* object is used to define the required heat transfer model that will evaluate heat transfer coefficient in the cylinders. *EngCylTWall* is used to set values for the temperatures of cylinder head, pistons and cylinder walls.

Since no measured swirl data was available for the EPTE engine, GT-Power™ recommended the use of *WoschniGT* model to determine the in-cylinder heat transfer coefficient [10]. The convective heat transfer coefficient for the *WoschniGT* model is:

$$h_{c(WoschniGT)} = 3.01426 * \frac{p^{0.8} w^{0.8}}{B^{0.2} T^{0.5}} \tag{3.11}$$

where, h_c is the convective heat transfer coefficient (in $W/m^2 * K$), B is the cylinder bore diameter (m), p is the cylinder pressure (kPa) and T is the cylinder temperature (K).

The data of cylinder wall temperatures were not available for the EPTE model yet. Hence, GT-Power™ recommended the following temperatures to be set in *'EngCylTWall'* object. Values are recommended for full load conditions [10]. The temperature values given below were used for both the combustion cylinders and the EXC component.

- Cylinder head temperature = 550-600K
- Cylinder piston temperature = 550-600K
- Cylinder wall temperature = 400K

3.3.4 Combustion modelling

GT-Power™ provides multiple modelling alternatives for combustion depending on the intention of the simulation and type of engine being modelled [Spark-Ignition (SI) or Compression-Ignition (CI)]. The three approaches to combustion modelling are:

- Predictive Modelling: A predictive model is used to study the effects of variables like injection timing, residual fraction that directly affect the combustion model parameters like burn rate. In this model, the burn rate is predicted from variables such as pressure, temperature, equivalence ratio etc. Cylinder geometry, spark timing and fuel properties are also taken into account. The predictive model requires a measured data to calibrate the simulation model in order to achieve accurate results.

- Non-Predictive Modelling: This model can be used to study variables in a simulation that has little influence on the burn rate. Burn rate is set as a simulation input rather than being predicted. As long as there is enough fuel available in the cylinder, burn rate inputted will be considered regardless of the cylinder geometry or injection timing.
- Semi-Predictive Modelling: It offers a good balance between the two models mentioned above. While this model is sensitive to variables that affect the burn rate, users can still impose burn rate as a simulation input with the help of lookup tables or other methods. Different neural networks are employed to predict the parameter values that are to be specified for non-predictive model. This is a more complex since it involves a lot of control systems [10].

As no measured data was available for EPTE simulation model in order to calibrate the combustion model, predictive model was not used. Semi-predictive method was discarded due to the simulation complexities and higher computational time. The non-predictive model provides a faster computation and is not affected by other variables in the simulation. Also, Weibe function is a zero-dimensional non-predictive combustion model most frequently used for gas exchange studies in SI engines.

The object *'EngCylCombSIWiebe'* is a SI Wiebe Model in which the Weibe function calculates an approximate profile of SI burn rate. This model is recommended by GT-Power$^{\text{TM}}$ to impose a reasonable burn rate when measured data of cylinder pressure is unavailable, as was the case in the current thesis. Wiebe constant, Start Of Combustion (SOC) and burn rate together constitute the Wiebe equations and are given by equations 3.12, 3.13 and 3.14. All equations were taken from GT-Power$^{\text{TM}}$ documentation [10].

Inputs:

- AA = Anchor Angle (deg)
- D = Duration (deg)
- E = Wiebe Exponent
- CE = Fraction of Fuel Burned (also known as "Combustion Efficiency")
- BM = Burned Fuel Percentage at Anchor Angle
- BS = Burned Fuel Percentage at Duration Start
- BE = Burned Fuel Percentage at Duration End

Calculated Constants:

- $BMC = -ln(1 - BM)$ is the Burned Midpoint Constant
- $BSC = -ln(1 - BS)$ is the Burned Start Constant
- $BEC = -ln(1 - BE)$ is the Burned End Constant

$$WC = \left[\frac{D}{BEC^{\frac{1}{(E+1)}} - BSC^{\frac{1}{(E+1)}}} \right]^{-(E+1)} \tag{3.12}$$

$$SOC = AA - \frac{(D)(BMC)^{\frac{1}{(E+1)}}}{BEC^{\frac{1}{(E+1)}} - BSC^{\frac{1}{(E+1)}}} \tag{3.13}$$

$$Combustion(\theta) = (CE)[1 - e^{-(WC)(\theta - SOC)^{(E+1)}}] \tag{3.14}$$

where, θ is the instantaneous crank angle. The cumulative burn rate calculated is normalized to unity [10].

Table 2 shows the values of different combustion model attributes used in baseline engine and EPTE simulation models. Some default parameter values are also mentioned below. Note that the notation "def" denotes the default values set in GT-Power™.

Table 2: *EngCylCombSIWiebe* object specifications

ATTRIBUTE	VALUE	UNIT
Anchor Angle (= 50% burn)	8.0	deg
Duration (= 10% to 90% burn)	25.0	deg
Wiebe Exponent	def (= 2.0)	
Fraction of Fuel Burned	1.0	$fraction$
Number of Temperature Zones	two-temp	
Burned Fuel % at Anchor Angle	def (= 50.0)	%
Burned Fuel % at Duration Start	def (= 10.0)	%
Burned Fuel % at Duration End	def (= 90.0)	%

3.3.5 Fuel injection

Fuel injection is done with the help of an object called *'InjConn'*. There are different kinds of *InjConn* objects depending on the type of combustion model used, type of fuel and the method of injection. In this thesis, the EPTE model required port-fuel sequential injection of gasoline fuel. Hence an object called *'InjAFSeqConn'* was used for both combustion cylinders. An attribute in this object, called "Vaporized Fuel Fraction", determines the fraction of liquid fuel that evaporates into vapour fuel upon injection [10]. GT-Power^{TM} recommends a value of 0.3 for a port-injected SI engine. An important parameter of *InjAFSeqConn* object is the pulse width; it is the duration of fuel injection in crank angle degrees. In order to estimate delivery rate of the injector, certain considerations are made if pulse width is not known. GT-Power^{TM} recommends that "the longest pulse duration in crank-angle degrees is about equal to the duration of the intake valve opening: 180 to 210 degrees" [10]. GT-Power^{TM} also recommends considering the highest engine speed while estimating injection delivery rate. The equation to calculate the delivery rate is given by:

$$\dot{m}_{delivery} = \eta_v \rho_{ref} N_{rpm} V_d (\frac{F}{A}) \frac{6}{\#Cylinders * PulseWidth} \tag{3.15}$$

where, $\dot{m}_{delivery}$ is the injector delivery rate (g/s), η_v is the volumetric efficiency (in fraction), ρ_{ref} is the reference density (kg/m^3) ($1.16 kg/m^3$, ambient conditions), N_{rpm} is the engine speed (RPM), V_d is the displacement of engine (in Litres), F/A is the fuel-to-air ratio & $PulseWidth$ is the duration of injection, in CAD [10].

The fuel used in this thesis was called 'Indolene'. It is the standard gasoline fuel used for engine testing purpose. Octane number of indolene is similar to commercially available gasoline fuels. Table 3 shows values of different friction model attributes used in baseline engine and EPTE engine models. In the table, "Injection Timing Angle" refers to the crank angle relative to Top-Dead-Center Firing (TDCF) at which fuel injection starts.

Table 3: *InjAFSeqConn* object specifications

ATTRIBUTE	VALUE	UNIT
Fluid Object	indolene-combust	
Injected Fluid Temperature	300	K
Vaporized Fluid Fraction	0.3	
Injector Location	0.5 (@ centre of inlet ports)	
Injection Timing Angle	360	CAD

3.4 Model Generation

The following section provides a detailed methodology for creating the EPTE model in GT-Power^{TM}. A basic understanding of this was provided in section 1.6. The EPTE concept presented by Olshammar in his patent [27] is still in the early stages of research; there was no physical engine model/prototype available to extract data for simulation purposes. However, GT-Power^{TM} provides a set of example models that are modelled based on the intention of simulation and certain default values of variables are pre-specified based on these purposes. One such example model was adopted in order to simulate and assess the technical potential of EPTE model. *'4cylSI-final'* is an example model which can be found under $Files \rightarrow Tutorials \rightarrow Modelling\_Applications \rightarrow 04 - 4cylSI$ in the GT-ISE software. The example model was modified based on requirement specifications by Olshammar, to create a baseline engine model and subsequently, the EPTE model. EPTE model was built from baseline engine model by adding an exhaust cylinder to the baseline engine model. Except for geometrical parameters and timing attributes (firing interval, valve timings) that were optimized for performance, all other engine attributes were kept constant between the two models. The multiphysics objects used (flow model, heat transfer model, friction model), solution algorithms and initialization settings were also unchanged. DOE studies were performed to determine the best ranges of operation for all optimizing parameters. This resulted in a fair comparison of performance metrics by limiting deviations between the models.

3.4.1 Baseline engine model

A pre-existing example *4cylSI-final* mentioned in Section 3.4 was imported into GT-Power^{TM}. This model was a four-cylinder naturally aspirated SI engine model. In order to meet the requirement specifications, two cylinders were removed from the model along with the associated intake manifold pipe components, exhaust manifold pipe components. This resulted in a two-cylinder naturally aspirated SI engine.

Table 4 gives a basic summary of engine configurations that apply for both baseline engine and EPTE models. Figure 14 represents the final baseline engine model. An enlarged view of figure 14 can be found in Appendix A.2. Exhaust ports of both *'cylinder-1'* and *'cylinder-4'* were connected to a common exhaust manifold via *'FlowSplitTRight-3'*. *FlowSplitTRight-3* is a T-shaped pipe component that combines exhaust flows from the two ports *'exhport-1'* and *'exhport-4'* to provide a common flow passage for the exhaust gases. Modelling of *FlowSplitTRight-3* is described in Appendix A.1. Orifices called *'OrificeConn'* in GT-Power^{TM} were used to connect any two pipes together. Part *'7'* is a rounded pipe that connects the exhaust manifold to the turbocharger arrangement.

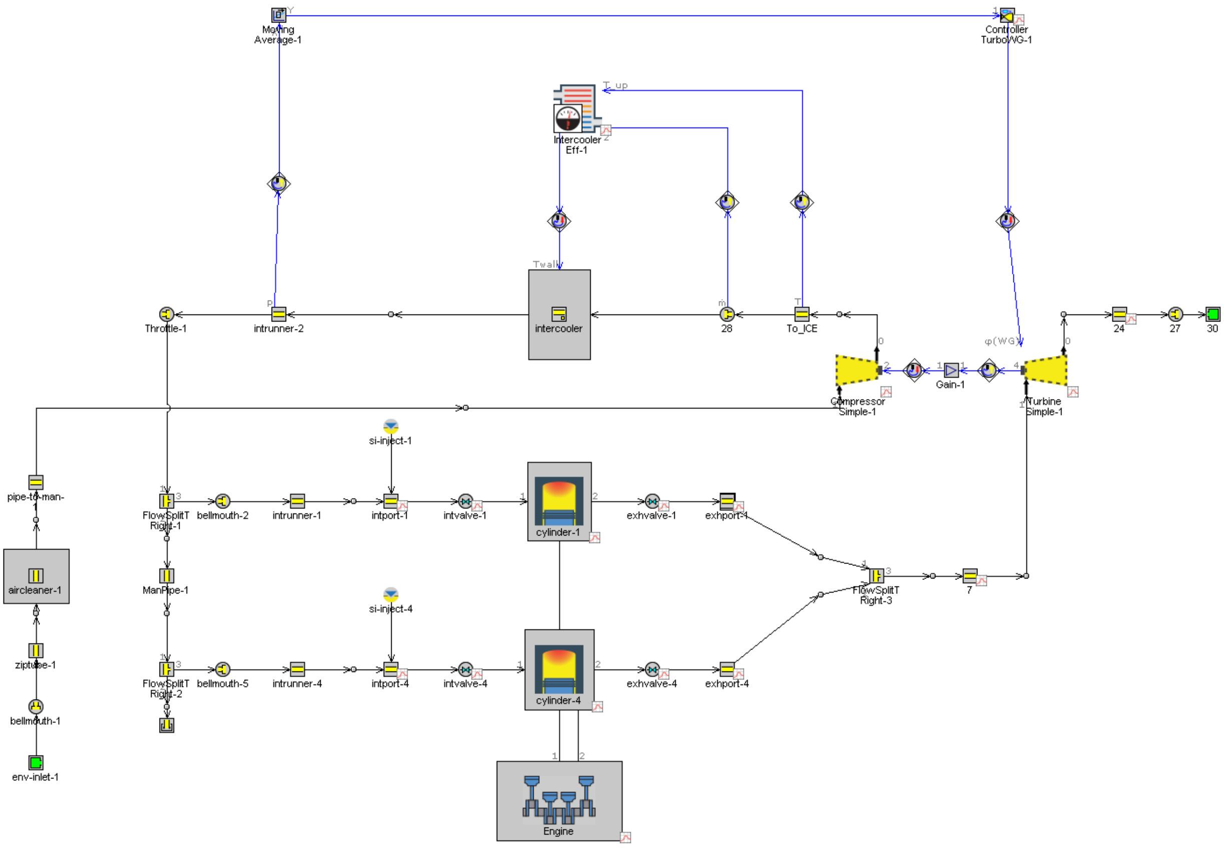

Figure 14: Baseline Engine Model

Table 4: Fundamental specifications of Baseline engine model

ATTRIBUTE	**VALUE**	**UNIT**
Engine Type	2-cylinder, four stroke, Inline	
Fuel Injection	PFI	
Engine Speed Range	2000-6500	rpm
Bore x Stroke	86 x 86.07	mm
Displacement Volume	1000	cc
Geometrical Compression Ratio	9.5	
Connecting Rod Length	175	mm
TDC Clearance Height	1.0	mm
Head/Bore Area Ratio	1.15	mm
Piston/Bore Area Ratio	1.0	mm

Initial fluid states

Table 5 gives values for the initial conditions of intake air and exhaust gases required to start the simulations. Object *'initial'* was used as initial fluid state for all components before the combustion cylinders and *'initial_exh'* was used for all components after, wherever applicable. The compositions *air* and *exh_gas* are available as reference objects in GT-Power^{TM}.

Table 5: Initial fluid state specifications

ATTRIBUTE	*initial*	*initial_exh*	UNIT
Pressure (Absolute)	1.0	1.1	bar
Temperature	300	750	K
Composition	air	exh_gas	

Fuel injectors

The fuel injector components are represented by *'si-inject-1'* and *'si-inject-4'*. The injectors were positioned at the centre of the intake ports *'intport-1'* and *'intport-4'*. The estimation of delivery rate was based on equation 3.15, GT-Power^{TM} recommendations mentioned in subsection 3.3.5 and engine specifications mentioned in table 4. Other specifications of the fuel injectors are mentioned in table 3.

Intake plenum

The intake plenum was modelled by three components: *'FlowSplitTRight-1'*, *'FlowSplitTRight-2'* and *'ManPipe-1'*. Volume of intake plenum was inputted as a multiple of the engine displacement volume. DOE studies were performed to estimate the volume of plenum. Simulations showed that plenum volume 6 times the volume of engine displacement (i.e., 6 litres in this case) improved engine performance, in both BSFC and BP. More details of DOE studies are mentioned in Appendix B.2.

Thermocouple

Thermocouple template from GT-Power^{TM} was used to measure temperatures in different sections of the engine model. The reference object *'thermocouple'* was used to model the thermocouples inside the pipes. Table 6 lists the specifications of *thermocouple*. All attribute values of *thermocouple* not mentioned below were considered as default.

Table 6: *Thermocouple* reference object specifications

ATTRIBUTE	VALUE	UNIT
Construction Type	Shielded	
Sheath Material	Steel	
Sheath Diameter	4.5	mm
Sheath Length	20.0	mm
Sheath Thickness	0.5	mm
Emissivity	0.15	

Turbocharger

There are different templates available in the software library to model the turbocharger arrangement. In the absence of a turbocharger map, GT-Power™ recommends using *TurbineSimple* and *CompressorSimple* templates as mentioned briefly in section 1.6. Turbocharger shaft was modelled as a sensor-actuator system with a gain controller. The system senses (part *'SensorConn'* the turbine power and rotates *CompressorSimple* using an actuator (part *'ActuatorConn'*). Gain controller *'Gain-1'* was set at 0.9 to account for shaft losses. GT-Power™ does not allow for a turbocharger shaft component to be attached when the *TurbineSimple* and *CompressorSimple* models are used.

TurbineSimple

This template represents a turbocharger's turbine in simple form. Basic understanding of the system was provided in the previous paragraph. Using turbine orifice flow model and imposed efficiency, it will estimate output power and temperature at the outlet. The flow rate of exhaust gases was computed by using upstream and downstream pressures. The pressure ratio, mass flow rate, and efficiency were used to calculate the output power. The pressure ratio and efficiency were also used to evaluate the outlet temperature. This template is meant to be used in the early phases of engine design when turbine maps aren't present; however the user wants to establish trends in a model which are similar to those seen in a turbocharged engine [14]. Inlet of *TurbineSimple* was connected to pipe component *7*, and the outlet was connected to environment. *TurbineSimple* has a built-in wastegate system, whose diameter was controlled by component *'ControllerTurboWG'*. An averaging signal was used to sense pressure in the intake manifold component *'intrunner-2'* present after the heat exchanger, represented by component *'intercooler'*. Depending on this pressure *ControllerTurboWG* limits boost pressure to a desired value by changing the wastegate diameter. Specifications of the *TurbineSimple* are listed in table 7. In this table, $[orificedia]$ denotes that the turbine orifice diameter is an attribute that was being optimized and hence the range of values considered for optimization will be mentioned further in section 3.5.2.

Table 7: *TurbineSimple* template specifications

ATTRIBUTE	VALUE	UNIT
Inlet Pressure Flag	total	
Outlet Pressure Flag	total	
Efficiency: PR Lookup Definition	same-as-map	
Performance Definition	Orifice Flow & Constant Efficiency	
Turbine Efficiency	0.7	$fraction$
Turbine Orifice Diameter	$[orificedia]$	mm

CompressorSimple

Using basic thermodynamic equations, mass flow rate and output temperature were derived from inlet temperature, pressure ratio, efficiency, and input power. *ActuatorConn* was used to actuate the input power derived from *SensorConn*. This essentially works as a turbocharger shaft. $[inputpower]$ in table 8 refers to this power derived from the turbine when simulations start. The outlet temperature was obtained using the inlet temperature, pressure ratio, and efficiency. The mass flow rate was calculated utilizing temperature change throughout the compressor and input power [13]. Specifications of *CompressorSimple* are listed in table 8.

Table 8: *CompressorSimple* template specifications

ATTRIBUTE	VALUE	UNIT
Inlet Pressure Flag	total	
Outlet Pressure Flag	static	
Efficiency: PR Lookup Definition	same-as-map	
Compressor Efficiency	0.72	$fraction$
Compressor Input Power	$[inputpower]$	mm
Damping Time Scale	1.0	ms

Intercooler

Intercooler is used to cool the compressed air coming from *CompressorSimple* to reduce temperature and increase density of intake air, prior to entering intake plenum. *Intercooler* was modelled as a heat exchanger with several rectangular pipes stacked parallelly, specifications mentioned in table 9. It has a coolant temperature of $310K$, effectiveness value of 0.9 at low air mass flow rate and 0.85 at higher flow rates. In order to effectively actuate the *intercooler* pipe gas outlet temperature, GT-Power^{TM} [9] recommends setting the part attribute "Heat Transfer Multiplier" in *'IntercoolerEff-1'* to a high value, say 50. This allowed sufficient heat transfer between the gas and *intercooler* pipes so that the *intercooler* gas outlet temperature achieved a value very close to pipe wall temperature.

Table 9: Specifications of *intercooler* component

PART ATTRIBUTE	VALUE	UNIT
Height at Inlet End (=Outlet End)	4	mm
Width at Inlet End (=Outlet End)	40	mm
Length	50	mm
Number of Identical Pipes	10	
Wall Temperature	Imposed @ 350	K

3.4.2 EPTE model

In order to model EPTE, minimal changes were made to the baseline engine model. The EXC in EPTE should be supplemental to existing engine designs and manufacturing processes. Any drastic deviation from the baseline engine would impact performance that may not allow for a fair comparison. Based on the requirement specifications, an EXC replaced the *FlowSplitTRight-3* component. In the context of GT-Power^{TM}, EXC is represented by the component *'PistonCylinder-1-1'*. The EPTE model is depicted in figure 15. An enlarged view of figure 15 can be found in Appendix A.2. *PistonCylinder-1-1* models a variable volume of a piston machine with no combustion, which aligns with the required properties of EXC mentioned in section 3.1. *PistonCylinder-1-1* was connected to the same engine crankshaft as the two combustion cylinders. It has two inlet ports, linked to the two exhaust channels *exhport-1* and *exhport-4*. Neither the inlet sides nor the outlet side features any valves. Outlet of the *PistonCylinder-1-1* connects to *TurbineSimple* via pipe *7*. Equations and specifications regarding multiphysics and solvers were unchanged; meaning, friction and heat transfer attribute values along with cylinder wall temperatures were equal in both EXC and the combustion cylinder. The firing order of the baseline engine was $1 - 2$ with a firing interval of 360 CAD. In the EPTE model, the firing order was $1 - EXC - 2$. Firing in the case of *PistonCylinder-1-1* means the start of expansion stroke from TDC to BDC. This is not to be confused with firing of the spark plug, as there is no combustion in *PistonCylinder-1-1* and consequently no fuel injection and spark ignition. Start of firing in the case of both the combustion cylinders 1 and 2 denotes the start of the power stroke which is when the the piston moves from TDC to BDC during the engine cycle. The firing angles (in *CAD*) for *cylinder-1*, *PistonCylinder-1-1* and *cylinder-2* were 0, $[fireint]$, and $(360 - [fireint])$ respectively. Cylinder firing angle was relative to the preceding cylinder. For the first cylinder, GT-Power^{TM} recommends setting this value as zero. $[fireint]$ denotes that this value was optimized. The cylinder geometry of EXC was same as the combustion cylinders except for the bore diameter and compression ratio; these two parameters, $[exhbore]$ and $[exh - CR]$ were optimized along with $[fireint]$. The parameters $[exhbore]$ and $[exh-CR]$ denotes the bore diameter and geometrical compression ratio of the EXC component respectively. The range of values considered during optimization is provided in table 12.

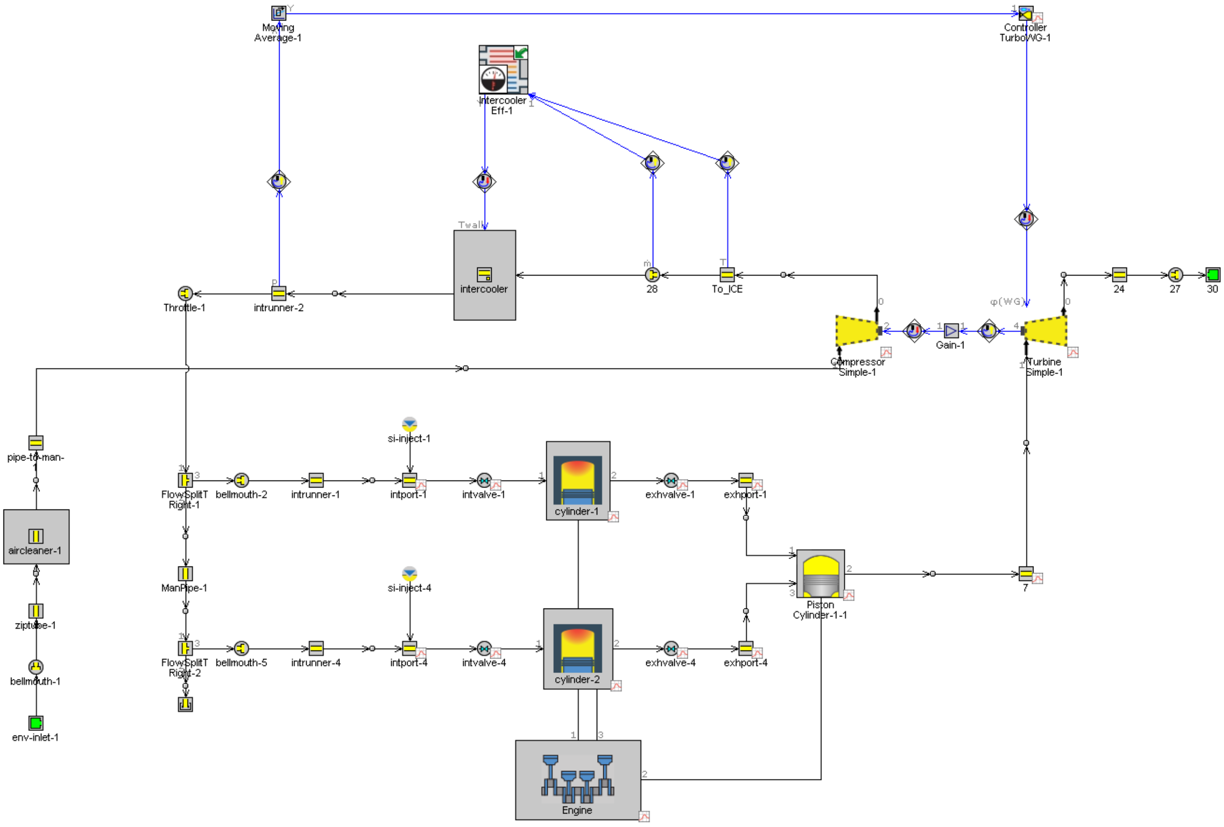

Figure 15: EPTE model

3.5 Model Optimization

This section discusses the optimization approach used for both the models: Baseline engine and EPTE. The optimization process was performed using the IDO tool in GT-Power^{TM} software. The optimized models emanating from this process were then used for the evaluation of performance metrics, gas exchange metrics and other critical indicators discussed in chapter 4. The following sub-sections will explain about the approach and techniques used for model optimization followed by the engine parameters which were optimized for both the baseline engine and EPTE. In the context of engine development activities within the transport industry, optimization of engine parameters is often referred to as “calibration”.

3.5.1 Optimization approach

This subsection explains the optimization approach which was adopted in the thesis project. To perform a fair comparison regarding various performance and gas exchange metrics, it was vital that the approach used for optimizing both the engine models were alike. This meant that the type of optimization, optimization algorithm and optimization objectives were the same for both the baseline engine and EPTE models. The motivation behind such optimization choices are also explained in this sub-section.

The background knowledge used for performing the optimization process via IDO emanated from Gamma Technologies’ Optimization Manual, 2019 version [12]. The optimizer feature in GT-Power^{TM} works based on an automated - iterative approach. This feature in the IDO sets input variables, runs the model, evaluates the model response variables, and changes the input variables again to achieve the optimization objective specified by the user. This process continues until a stopping criteria is met [12]. In this context, the response variables were BSFC and BP.

In this thesis project, the optimization process involved two objectives. One objective was to minimize the BSFC and the other one was to maximize the BP across the operating engine speed range. Therefore, a multi-objective optimization approach was used in this concept assessment study. These objectives were based on a case-weighted average. This means that the two objectives were given a certain weightage factor for engine speed cases ranging from 2000 RPM to 6500 RPM. Within an operating range of 2000 RPM to 5500 RPM, 40 % weightage was given to BP maximization and 60 % weightage was assigned for BSFC minimization. For engine speeds of 6000 RPM and 6500 RPM, 40% weightage was given to BSFC minimization and 60% weightage was given to BP maximization. There are two sub-approaches under multi-objective optimization in GT-Power^{TM} IDO. One is the weighted-sum approach and the other one is called as the pareto approach. According to GT-Power^{TM} optimization manual [12], weighted-sum approach is a reasonable method when the multiple objectives involved in the optimization process decrease or increase simultaneously when the factor values change. The factor values are the system variables which are to be optimized to achieve the objectives specified by the user. However, a major number of optimization problems in the field of engineering design incorporate trade-offs, for which the weighted-sum approach would not be a feasible method. In such scenarios, the pareto approach under multi-objective optimization is recommended [12]. Therefore, multi-objective optimization with pareto approach was used in the optimization process of both the baseline engine and EPTE models. This choice would help to maintain an adequate level of internal validity, as compared to the weighted-sum approach.

There are various search algorithms available in the GT-Power^{TM} optimization tool. According to the optimization manual [12], Genetic Algorithm (NSGA - III) and Covariance Matrix Adaptation Evolution Strategy (CMAES) are recommended for optimization problems with medium-high complexity. These algorithms are predominantly used when the relationship between the factor values and the response variables is non-linear, and when there are more than four factor values involved. However, the optimization manual further recommends the genetic algorithm over CMAES for multi-objective optimization problems. Therefore, genetic algorithm was used for the model optimization in the thesis project.

Table 10 provides the specifications related to the genetic algorithm used for optimizing the two engine models. It must be noted that the specifications highlighted in the table below were the same while optimizing both the engine models.

Table 10: Specifications of genetic algorithm

ATTRIBUTE	**OBJECT VALUE**
Population Size	def (=calculated)
Number of Generations	def (=15)
Crossover Rate	def (=1)
Crossover Rate Distribution Index	def (=15)
Mutation Rate	def (=calculated)
Mutation Rate Distribution Index	def (=20)

From the table 10, all values related to the attributes were fed based on the default or the recommended values by Gamma Technologies in their optimization manual [12]. However, the most critical attributes regarding the optimization process were population size and number of generations. The number of design conditions evaluated in the model optimization is a direct function of these two attributes. Equation 3.16 describes this relationship.

$$\text{No. of designs evaluated} = \text{Population size} \times \text{No. of generations} \tag{3.16}$$

The attribute ”population size” in equation 3.16 depends on the number of engine factors to be optimized [12]. According to the GT-Power^{TM} optimization manual [12], the population size is 50 if the number of factor values is greater than 9. During the optimization of both the engine models, the number of factor values optimized was greater than 9. These engine factor values have been highlighted in sub-sections 3.5.2 and 3.5.3. Therefore, the population size was calculated as 50. As a result, the total number of design conditions evaluated by the IDO was 750. This number corresponded to both the engine models. After performing the genetic algorithm-based optimization, the optimization tool in GT-Power^{TM} recommended some optimized models out of all the 750 design conditions. These optimized models encapsulated both local and global optimums. But GT-Power^{TM} specifies that it is impossible for any optimizer to identify the optimized model which represents the global optimum. Therefore, the user has to search through the entire design space of the optimized models and thereafter decide the most suitable optimized model based on some subjective information. Therefore, a subjective-based framework was adopted for selecting the most suitable optimized model within the optimization process. This framework is highlighted in subsection 3.5.4.

3.5.2 Baseline engine model optimization

This sub-section highlights and discusses the engine variables or factors which were optimized for the baseline engine model. The range for each of these variables which was used as an input for the optimization tool has been specified. This range was decided based on DOE studies which yielded reasonably low BSFC values and high BP values across the operating range. More information about the DOE studies has been explained in Appendix B.2. The optimization approach discussed in subsection 3.5.1 was followed during the calibration of baseline engine model. Table 11 lists all the engine variables, their corresponding part name according to figure 14 and the range considered for the variables during the optimization process.

Table 11: Engine variables optimized for baseline engine model

ENGINE VARIABLE	PART NAME	RANGE	UNIT
Intake Runner Length	*intrunner-1*, *intrunner-4*	300-700	mm
Intake Runner Diameter	*intrunner-1*, *intrunner-4*	33-80	mm
Intake Valve Opening (IVO)	*intvalve-1*, *intvalve-4*	300-360	CAD
Intake Valve Opening Duration	*intvalve-1*, *intvalve-4*	150-300	CAD
Fuel Injection Rate	*si-inject-1*, *si-inject-4*	18-40	g/s
Exhaust Port Length	*exhport-1*, *exhport-4*	30-70	mm
Exhaust Port Diameter	*exhport-1*, *exhport-4*	30-70	mm
Exhaust Valve Opening (EVO)	*exhvalve-1*, *exhvalve-4*	102-140	CAD
Exhaust Valve Opening Duration	*exhvalve-1*, *exhvalve-4*	220-320	CAD
Exhaust Runner Diameter	*Pipe-Round 7*	30-80	mm
Exhaust Runner Length	*Pipe-Round 7*	30-80	mm
Exhaust Split Chamber Length	*FlowSplitTRight-3*	30-70	mm
Turbine Orifice Diameter	*TurbineSimple-1*	15-40	mm

3.5.3 EPTE model optimization

This sub-section highlights and discusses the engine variables or factors which were optimized for the EPTE model. The range for each of these variables used as an input for the optimization tool have been specified. This range was decided based on DOE studies which yielded reasonably low BSFC values and high BP values across the operating range. More information about the DOE studies has been explained in Appendix B.2. The optimization approach discussed in subsection 3.5.1 was followed during the calibration of EPTE model. Table 12 lists all the engine variables, their corresponding part name according to figure 15 and the range considered for the variables during the optimization process. It must be noted that the component *FlowSplitTRight-3* was replaced by *PistonCylinder-1-1* in the EPTE model as discussed in subsection 3.4.2. Therefore, parameters like bore diameter, geometrical compression ratio and firing interval for the EXC component were optimized instead. All other engine variables specified in table 11 were optimized in the EPTE model as well. Table 12 has been depicted in the following page.

Table 12: Engine variables optimized for EPTE model

ENGINE VARIABLE	PART NAME	RANGE	UNIT
Intake Runner Length	*intrunner-1*, *intrunner-4*	300-700	mm
Intake Runner Diameter	*intrunner-1*, *intrunner-4*	33-80	mm
Intake Valve Opening (IVO)	*intvalve-1*, *intvalve-4*	300-360	CAD
Intake Valve Opening Duration	*intvalve-1*, *intvalve-4*	150-300	CAD
Fuel Injection Rate	*si-inject-1*, *si-inject-4*	18-40	g/s
Exhaust Port Length	*exhport-1*, *exhport-4*	30-70	mm
Exhaust Port Diameter	*exhport-1*, *exhport-4*	30-70	mm
Exhaust Valve Opening (EVO)	*exhvalve-1*, *exhvalve-4*	102-140	CAD
Exhaust Valve Opening Duration	*exhvalve-1*,*exhvalve-4*	220-320	CAD
Exhaust Runner Diameter	*Pipe-Round 7*	30-80	mm
Exhaust Runner Length	*Pipe-Round 7*	30-80	mm
Turbine Orifice Diameter	*TurbineSimple-1*	15-40	mm
EXC Bore Diameter	*PistonCylinder-1-1*	70-115	mm
EXC Compression Ratio	*PistonCylinder-1-1*	5-50	No Unit
EXC Firing Interval with respect to Cylinder-1	*PistonCylinder-1-1*	100-200	CAD

3.5.4 Model evaluation

After the IDO tool suggested a set of optimized models for both the baseline engine and EPTE, a subjective-based framework was adopted to select the most suitable optimized model for both the engines. This framework was based on the following requirements:

1. The most suitable optimized model should have minimum BSFC values within an operating range of 2000 RPM to 5500 RPM, as compared to other optimized models.

2. The same optimized model should have maximum BP values for engine speeds of 6000 RPM and 6500 RPM, compared to other optimized models recommended by the optimization tool in GT-Power^{TM}. It must be noted that the engine speed range had an interval size of 500 RPM for both the optimization and the evaluation process concerning performance and gas exchange metrics.

This identification process behind selecting the most suitable optimized model for both the baseline engine and EPTE was performed independently. This means that the selection was not done parallelly, but rather in sequence for both the engine models. Such a practice ensured a fair and unbiased selection strategy, to enhance the internal validity of the results. After this process was completed, the selected models for both the baseline engine and EPTE were ready for post-processing and analysis.

Data concerning the response variables and other emanating engine variables from the final selection process was exported to Microsoft Excel for in-depth analysis of the performance and gas exchange metrics across the operating engine speed range. For quantifying the contribution of the EXC component towards the total BP produced at the crankshaft, the friction parameters from table 1 were used. These friction parameters were same for both the combustion cylinders and EXC component. Using the friction parameters, cylinder geometry and combustion cylinder peak pressure values, the BP was calculated for each combustion cylinder for all engine speeds under consideration. Subsequently, the brake power produced by the EXC component was calculated by subtracting the BP produced by the combustion cylinders from the total BP produced at the crankshaft. The results concerning overall performance and gas exchange metrics have been discussed in the subsequent chapter.

Chapter 4

Results

In this chapter, the most critical results are discussed and analyzed for the baseline engine and EPTE models after the optimization process. It compares the performance and critical gas exchange metrics of EPTE with the baseline engine model. Other results discussed are the exhaust cylinder's contribution to total brake power, predicted hardware modifications and normalized brake torque. All results analyzed were based on the background knowledge, theoretical frame-of-reference and the modelling approach used in GT-Power^{TM}.

4.1 Performance Metrics

This section presents the results obtained from the optimization simulations of baseline engine and EPTE models. Comparison was done between both the engine models based on the performance metrics such as BSFC and BP. This comparative analysis was done at different limits of intake boost pressures: 1.5 bar, 2.5 bar and 3.5 bar. The limit in the intake boost pressure of a turbocharged engine depends on the application area, and hence it was important to get an overall sense on how the performance metrics would vary with the intake boost pressure requirement and limits, for the EPTE model. The performance analysis was conducted across a broad operating range: 2000-6500 RPM.

4.1.1 Brake Specific Fuel Consumption (BSFC)

This performance metric is an indicator of fuel efficiency of an ICE, which produces shaft power using the burned fuel. BSFC is a typical performance indicator which helps to compare the fuel efficiency of engines with a power output. It is the ratio of the fuel consumption rate to the power output produced at the flywheel. Lower BSFC is a target which engine developers aim for, as it indicates better fuel economy and thereby relatively lower CO_2 emissions from the tailpipe. Figure 16 consolidates the changes in BSFC (in % terms) as a function of engine speed for different intake boost pressure limits. This change in BSFC is with respect to the baseline engine model. The intake boost pressure limits in bar is in absolute terms. The following comparison was done for both the models of baseline engine and EPTE after the optimization process. This was done to facilitate a fair comparison.

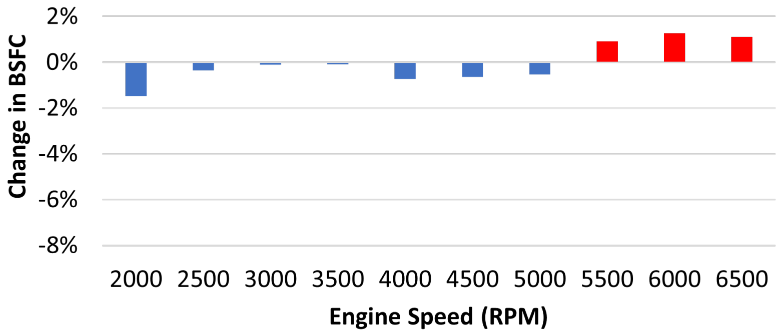

(a) @ 1.5 bar max. boost pressure

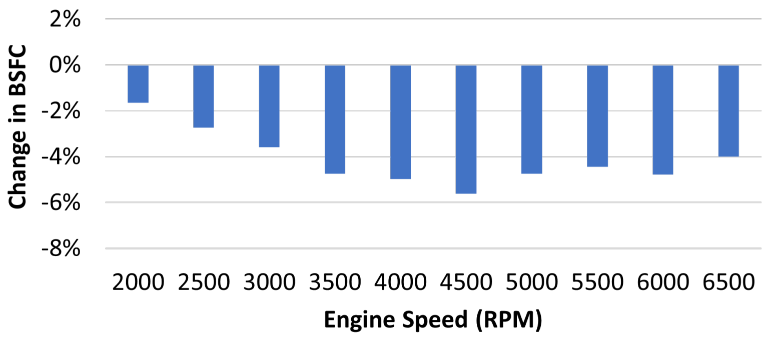

(b) @ 2.5 bar max. boost pressure

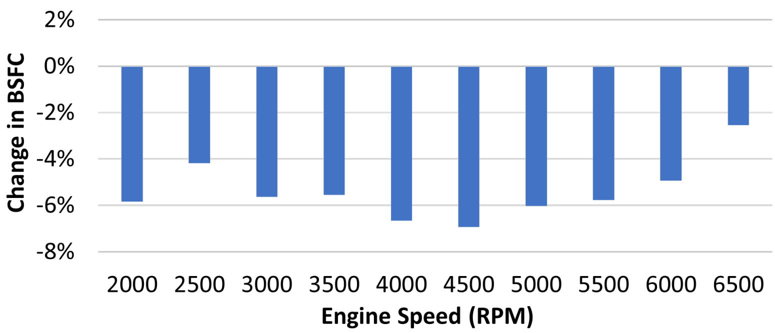

(c) @ 3.5 bar max. boost pressure

Figure 16: Change in BSFC v/s Engine Speed @ different boost pressure limits

From figure 16, it is conclusive that maximum reduction in BSFC is observed at higher intake boost pressure limits. At an intake boost pressure limit of 1.5 bar, the EPTE concept performed worse than the baseline engine at the higher RPM i.e. from 5500-6500 RPM. Furthermore, the reduction in BSFC at 1.5 bar maximum boost pressure was very minimal for the EPTE model from low to mid RPM. At intake boost pressure limits of 2.5 bar and 3.5 bar, the EPTE model performed better than the baseline engine model across the whole operating range, with the percentage reduction in BSFC amplified when the limit of intake boost pressure was increased from 2.5 bar to 3.5 bar. It is also interesting to note that the maximum reduction in BSFC occured at 4500 RPM when the comparison was done at 2.5 bar and 3.5 bar of intake boost pressure limits. The reason behind this is explained in section 4.3.

4.1.2 Brake Power (BP)

This performance indicator denotes the useful power produced at the crankshaft. From a realistic standpoint, a portion of the BP is used to deliver power to engine auxiliaries such as oil pump, water pump, camshaft, alternator etc. The remaining portion of the brake power is used to drive the wheels via the transmission. It should be noted that BP is the product of brake torque and the engine speed. Alternatively, it is also the remaining portion of the power produced inside the engine cylinders after the frictional losses that take place while the piston transfers the mechanical energy to the crankshaft, via the connecting rod.

Figure 17 consolidates the changes in BP (in % terms) as a function of engine speed for different intake boost pressure limits. This change in BP is with respect to the baseline engine model. The comparison between both the engine models was done after the optimization process to execute it from an equitable perspective. Furthermore, the friction parameters of the cylinders and pipes for both the baseline engine and EPTE models were unchanged throughout the simulation process. This was done to make sure that these effects are isolated while the comparison took place. Figure 17 is depicted in the succeeding page.

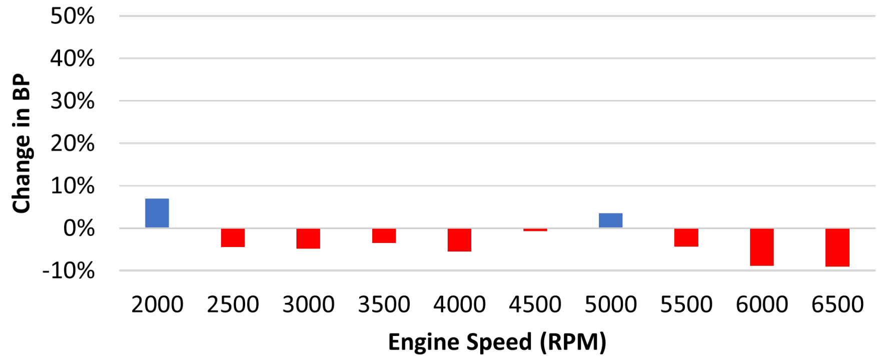

(a) @ 1.5 bar max. boost pressure

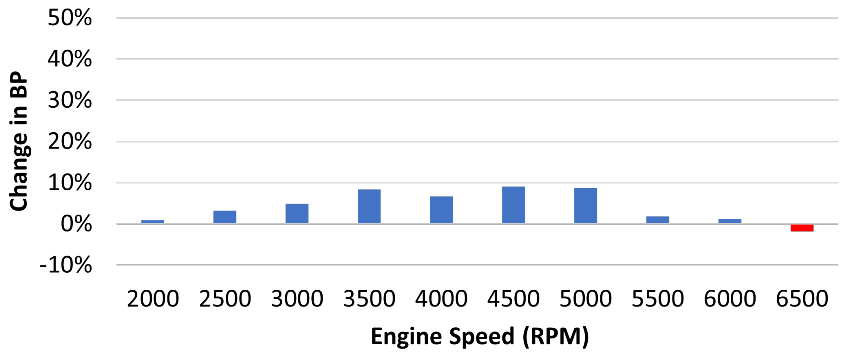

(b) @ 2.5 bar max. boost pressure

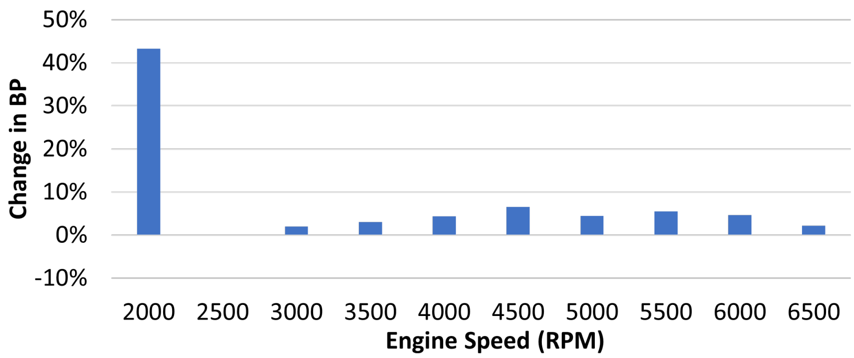

(c) @ 3.5 bar max. boost pressure

Figure 17: Change in BP v/s Engine Speed @ different boost pressure limits

It was observed that the EPTE concept performed worse than the baseline engine model even from the BP perspective, at an operating boost pressure limit of 1.5 bar. The performance from the BP standpoint improved in the EPTE model when the boost pressure limit was increased to 2.5 bar. At the highest operating boost pressure limit i.e. 3.5 bar, EPTE model exhibited better BP response across the whole operating RPM range. At 4500 RPM, EPTE concept proved to be around 7% more powerful than the baseline engine. At 2500 RPM, the BP improvement was just 0.12 %, and therefore it does not seem to be visible in the plot due to the scaling based on the minimum and maximum values. It must be noted that 43% increment in BP at 2000 RPM with the EPTE concept was observed because the optimization process yielded a turbine orifice diameter of 22 mm and 25 mm for the EPTE model and the baseline engine model respectively. The smaller turbine orifice diameter for the EPTE model indicated that the turbocharger spools up earlier in the operating range, compared to the baseline engine model. The faster spooling up of the turbine in the new concept increased the BP abruptly, unlike the scenario in baseline engine.

4.2 Gas Exchange Metrics

This section compares both the baseline engine and EPTE models based on gas exchange metrics. The gas exchange metrics under interest are: Crank-resolved pressure before and after the turbine. These metrics are explained in the subsections 4.2.1 and 4.2.2. From section 4.1, it was concluded that EPTE concept performs better than the baseline engine model across the whole operating range when the boost pressure limit is set to 3.5 bar. Therefore, the plots related to the critical gas exchange metrics are shown for the engines operating at 3.5 bar maximum boost pressure.

4.2.1 Crank-resolved pressure before turbine

This subsection deals with the comparison between the two engine models based on crank-resolved pressure plots before the turbine. This pressure is measured at part number 7 according to figures 14 and 15. Part number 7 is an exhaust runner connected to the turbine inlet. The pressure plots are static pressure measurements in absolute terms.

The motive behind comparing the pre-turbine pressure plots for both the engine models was to assess if the EPTE model facilitates in enhancing the degree of evenness in the exhaust pulse which enters the turbine. This would help to confirm the claim cited in Olshammar's patent [27]. This comparison is shown in figure 18, in the succeeding page.

Figure 18 consolidates the pressure measurements before the turbine, for both the models: Baseline engine and the EPTE. It must be noted that the plots in figure 18 have been imported from GT-Power^{TM}. In this figure, "Olshammar engine" corresponds to the EPTE model. The crank-resolved pressure plot typically depicts the pressure variation across the whole engine cycle i.e. across all the four strokes of the cycle. The x-axis in the plots which represents all the strokes of the engine cycle, was referenced as per the first combustion cylinder.

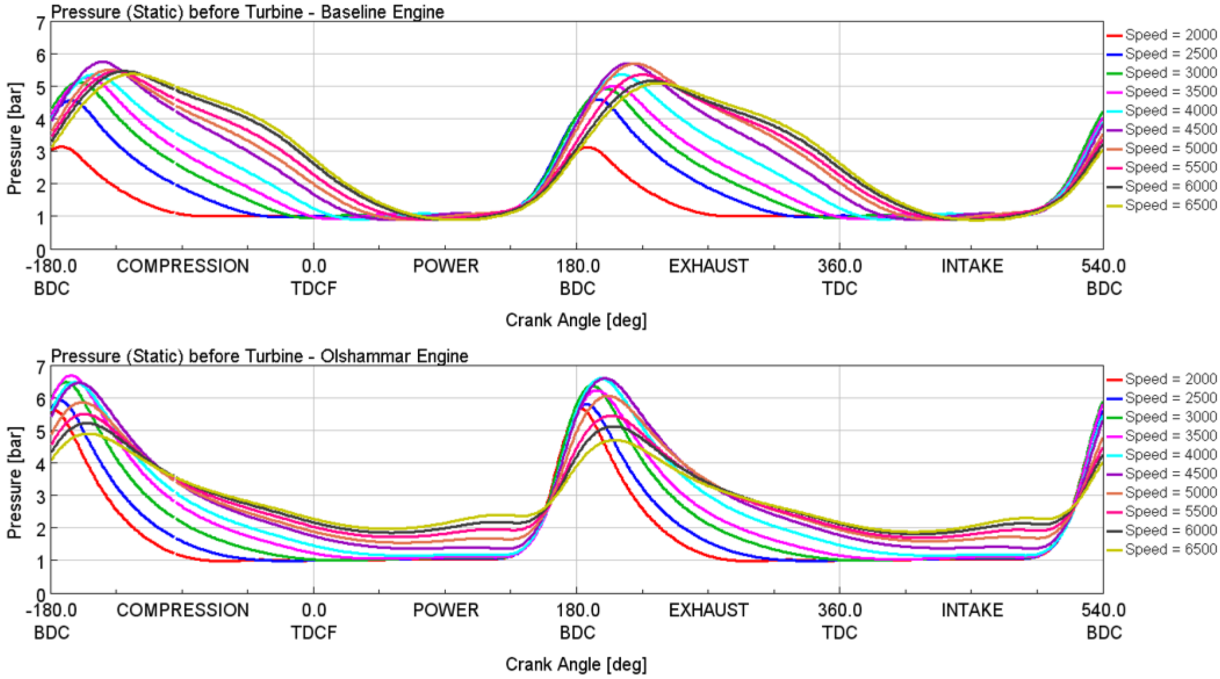

Figure 18: Crank-resolved pressure before turbine - Baseline engine and EPTE (Olshammar)

The first combustion cylinder is represented by ”cylinder-1” as per figures 14 and 15. Figure 18 depicts the exhaust pressure trace at all operating conditions, ranging from 2000 RPM to 6500 RPM. It must be noted that in the baseline engine model, the pressure trace is more uneven across the engine cycle, as compared to the EPTE model. This is because the pressure trace coincides with 1 bar and values under it for the baseline engine model, during the major portion of power and intake strokes. This indicated that there was no extra pressure on the turbine during these portions of the power and intake stroke, as the ambient pressure was set to atmospheric i.e. 1 bar. In the case of EPTE model or Olshammar engine model, the pressure trace hardly coincides with 1 bar. In most of the operating engine speeds, the exhaust pressure trace is above 1 bar for the whole duration of power and intake strokes. This indicated that the turbine in the EPTE model is subjected to an extra pressure across the engine cycle. This extra pressure on the turbine implied that there is more evenness in the exhaust pressure before the turbine, thereby creating a more uniform turbine power distribution across the engine cycle. From such an analysis, it was clear that the EPTE model increased the efficiency of the turbocharger, unlike the baseline engine model.

4.2.2 Crank-resolved pressure after turbine

This subsection deals with the comparison between the two engine models based on crank-resolved pressure plots after the turbine. This pressure is measured at part number 24 according to figures 14 and 15. Part number 24 is an exhaust runner with one end connected to the turbine outlet, and the other end linked to the atmosphere. It must be noted that the pressure plots are static pressure measurements in absolute terms.

The motive behind comparing the post-turbine pressure plots for both the engine models was to assess the effect of the EXC on the muffler and aftertreatment sizing and weight. Reduction in the size of such exhaust regulator components can also contribute to back-pressure reduction, thus maintaining better fuel economy levels.

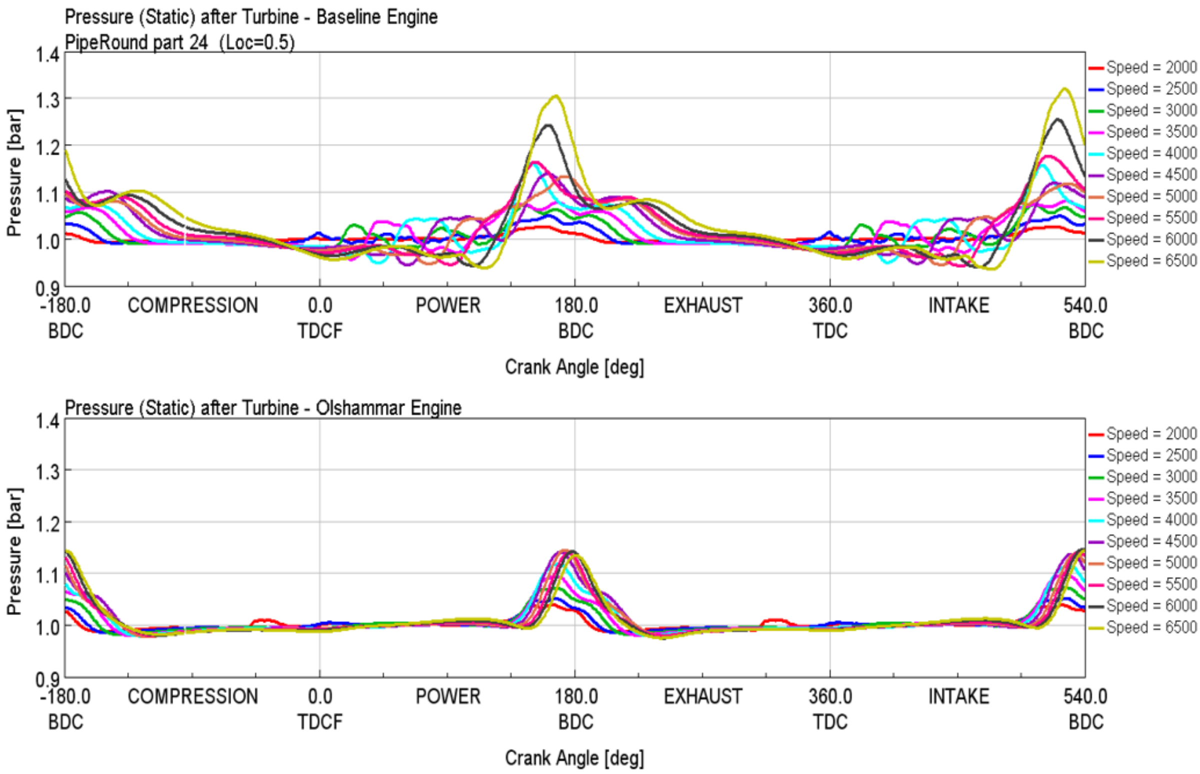

Figure 19: Crank-resolved pressure after turbine - Baseline engine and EPTE (Olshammar)

Figure 19 consolidates the pressure measurements at the turbine outlet, for both the models: Baseline engine and the EPTE. From the plots, it was observed that the exhaust pressure trace had higher peaks and higher flutter in the baseline engine, when compared against the EPTE concept. The design and overall size of exhaust regulator sub-systems such as mufflers and aftertreatment devices depend on the pulsating nature of the exhaust gas exiting the tailpipe. The EPTE concept exhibited lower peaks and lesser fluttering nature of the exhaust gas across the whole engine cycle and operating RPM range. Therefore, it could be inferred that a more compact and lower weight exhaust system could be designed and integrated with the turbine outlet.

4.3 Exhaust Cylinder (EXC) Contribution to Total BP

This section discusses the portion of total BP contributed by the EXC. This analysis was done at intake boost pressure limits: 1.5 bar, 2.5 bar and 3.5 bar. The motive of this section is to analyze as to what extent the EXC contributes to power generation using the fact that a portion of the exhaust gas flushing out of the combustion cylinders would exert gas pressure on the exhaust piston. The exhaust piston corresponds to the piston in the EXC. Figure 20 consolidates the plots which depict the percentage of total BP at the crankshaft which was contributed by the EXC, at different limits of boost pressure. The specifications of the EXC component which yielded these results are discussed in section B.1.

Based on Olshammar's patent [27], a portion of the exhaust gas emanating from the two firing cylinders push the piston in the EXC, whereas the remainder portion of the exhaust gas flows directly to the turbocharger via the outlet (17) of the EXC, based on figure 10. To have a better understanding of the BP contribution by the EXC, it was also vital to visualize the Pressure-Volume (PV) trace inside the EXC. This is depicted in figure 21. The PV trace is shown for all operating RPM.

Figure 20 has been depicted in the following page. From figure 20, it can be observed that there was a marginal contribution by the EXC towards the total BP produced at the crankshaft, when the EPTE concept operated at the minimum boost pressure limit under consideration, i.e., 1.5 bar. Furthermore, there was negative contribution from the EXC at the lowest and the highest RPM within the 1.5 bar boost pressure limit. At 2500 RPM, the contribution from the EXC component was around 0.01 %. Therefore the bar is not visible due to the scaling based on the minimum and maximum values. At 2.5 bar and 3.5 bar maximum boost pressure limits, the EXC component contributed to around 5% and 7% respectively, towards the total BP produced. These values corresponded to 4500 RPM, where the maximum contribution was observed. This is explained further by figure 21.

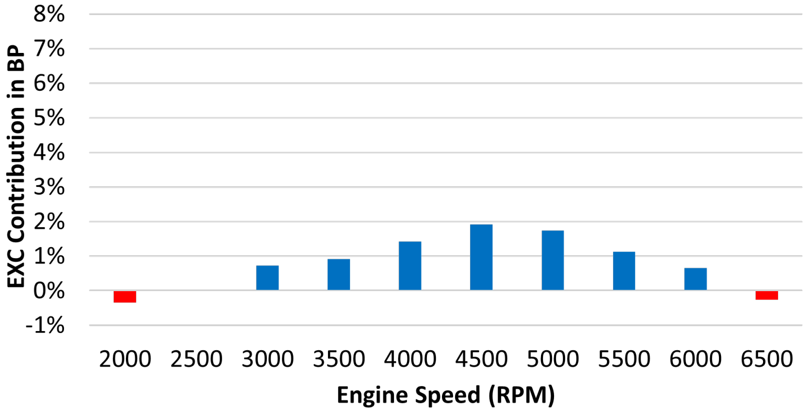

(a) @ 1.5 bar max. boost pressure

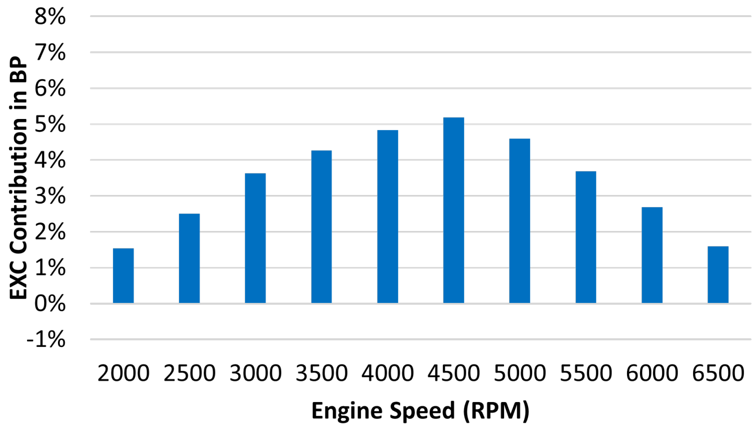

(b) @ 2.5 bar max. boost pressure

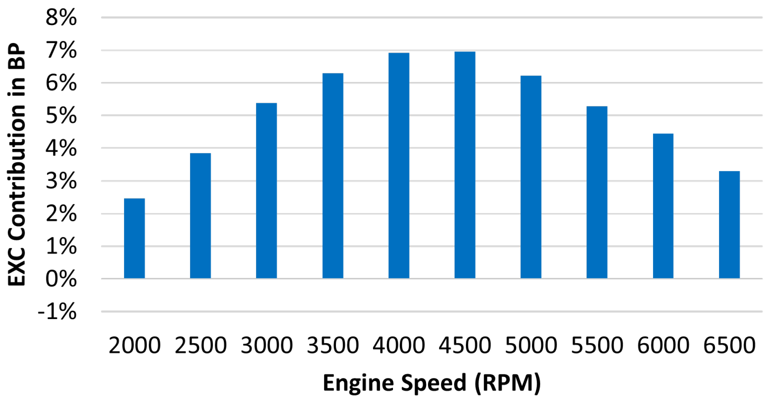

(c) @ 3.5 bar max. boost pressure

Figure 20: EXC Contribution in BP v/s Engine Speed @ different boost pressure limits

Figure 21 depicts the full PV trace inside the EXC component of the EPTE concept at 3.5 bar boost pressure limit. It has been specifically shown for 3.5 bar maximum boost pressure because the maximum contribution from the EXC occured at this operating condition. This PV trace was imported from GT-Power^{TM} simulations. It must be noted that each RPM shows two lines in the trace, as these represent full 720 degrees across the engine cycle. The area inside the PV trace is directly proportional to the BP contributed by the EXC component. Furthermore, the largest area enclosed by the PV trace was observed at 4500 RPM, represented by the darkened violet lines. Therefore, the maximum contribution towards the total BP occured at 4500 RPM, as shown in figure 20. Another important observation was that the peak pressures were quite low inside the EXC component, which indicated that this extra component could be manufactured with light-weight and less sophisticated materials during the prototype building activity of the EPTE. The peak pressure inside the EXC component was around 3.3% of the peak pressure inside the combustion cylinders.

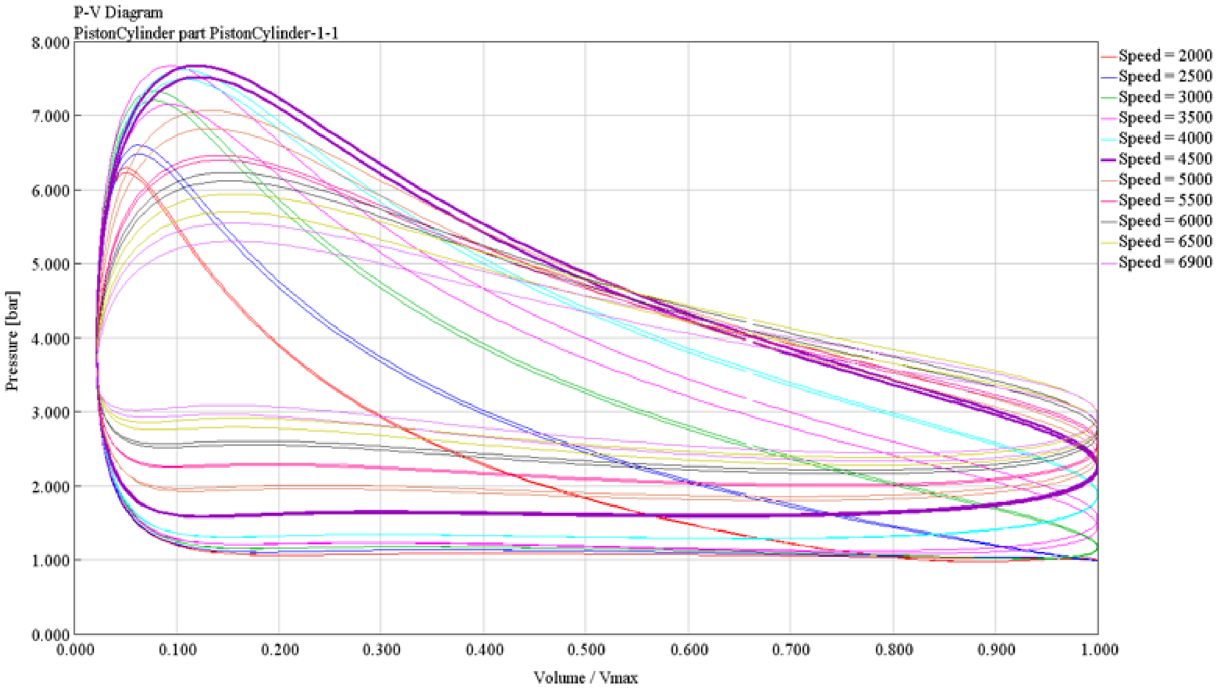

Figure 21: PV trace in EXC at 3.5 bar boost pressure limit

4.4 Predicted Hardware Modifications

This section discusses the predicted hardware modifications required while translating the baseline engine to the EPTE. These predictions in the hardware modifications were analyzed for the optimized models of both the engines. Based on section 4.1, it was inferred that EPTE model performed better than the baseline engine model both from the fuel consumption and power output standpoint, at the higher boost pressure limits of 2.5 bar and 3.5 bar. Thus, it was also vital to have a broad understanding of the extent to which the baseline engine should be modified apart from adding the EXC component, to produce such benefits. The change in the dimensions predicted in percentage terms was based on the intake and exhaust geometrical parameters which were suggested for both the engine models after the model optimization process.

4.4.1 Intake side

In the thesis project, the predicted modifications in the intake side dealt with the potential changes in intake runner length and intake runner diameter for the EPTE model relative to the baseline engine model. The intake plenum chamber volume was set to be six times the total engine displacement of the cylinders with combustion, for both the models: Baseline engine and EPTE. This was done to ensure that there was an adequate level and even distribution of air to the combustion cylinders. According to figures 14 and 15, the plenum chamber represented the combined volume of parts *FlowSplitTRight-1*, *ManPipe-1* and *FlowSplitTRight-2*. According to figure 14, the intake runner length represented the combined length of the components *intrunner-1* and *intport-1* for *cylinder-1*, and *intrunner-4* and *intport-4* for *cylinder-2*. It must be noted that the length of intake runners for each combustion cylinder were equal. Similarly for figure 15, the intake runner length represented the combined length of the components *intrunner-1* and *intport-1* for *cylinder-1*, and *intrunner-4* and *intport-4* for *cylinder-4*. Even for the EPTE model, the intake runner lengths for each combustion cylinder were equal. The intake runner diameter represented the diameter of the aforementioned components corresponding to the baseline engine and EPTE model. For both the engine models, the intake runner diameter was constant from the plenum chamber to the combustion cylinders. The diameter of intake runners for each combustion cylinder were equal in the respective engine models.

Figures 22 and 23 represent the relative changes in the intake runner length and intake runner diameter for the EPTE model with respect to the baseline engine model. These changes were predicted for the optimized models of baseline engine and EPTE for boost pressure limitss of 1.5 bar, 2.5 bar and 3.5 bar.

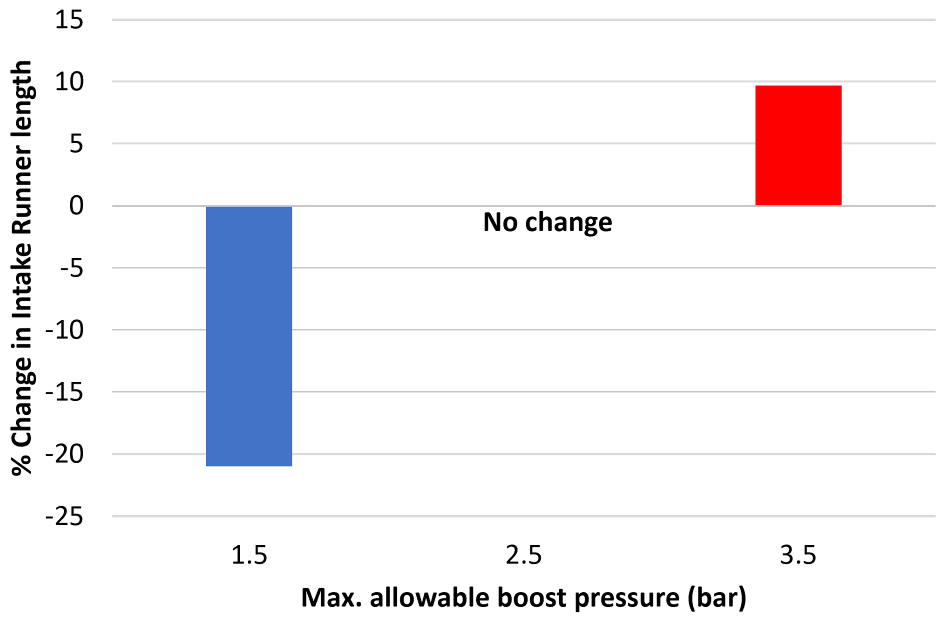

Figure 22: Change in Intake Runner Length v/s Boost Pressure Limit

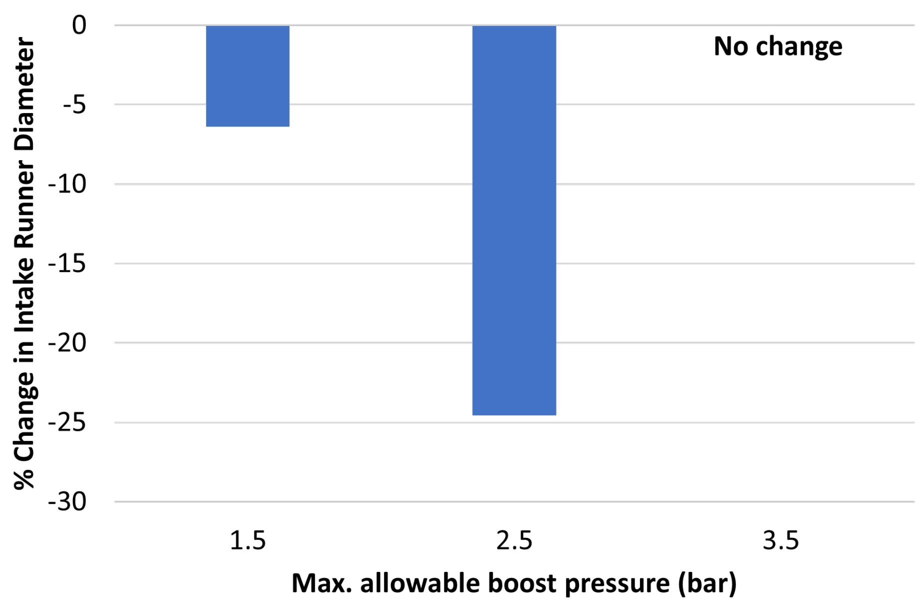

Figure 23: Change in Intake Runner Diameter v/s Boost Pressure Limit

Section 4.1 indicated that the EPTE model performed worse than the baseline engine model at 1.5 bar boost pressure limit, from the BSFC and BP standpoint. Therefore, dimensional reductions at 1.5 bar for the EPTE model depicted in figures 22 and 23 do not serve as a purpose of this section's analysis. At boost pressure limit of 2.5 bar, there was no change in the intake runner length in the EPTE model, as indicated by figure 22. This implied that the EPTE can be operated with the same intake runner length as the baseline engine, to produce the benefits highlighted in section 4.1. At the same boost pressure limit, the optimized EPTE model exhibited around 10% increase in the intake runner length, compared to the baseline engine model.

According to figure 23, the EPTE model exhibited the benefits discussed in section 4.1 with around 20 % narrower intake runner at a boost pressure limit of 2.5 bar. With an operating maximum boost pressure of 3.5 bar, the EPTE model exhibited benefits highlighted in section 4.1 with the same dimensions of intake runner diameter as the baseline engine model.

4.4.2 Exhaust side

In the thesis project, the predicted modifications in the exhaust side dealt with the potential changes in exhaust port length, exhaust port diameter, exhaust runner length, exhaust runner diameter and turbine orifice diameter for the EPTE model, relative to the baseline engine model. It must be note that these changes were measured for the optimized versions of the EPTE model against the optimized baseline engine models at different limits of boost pressure.

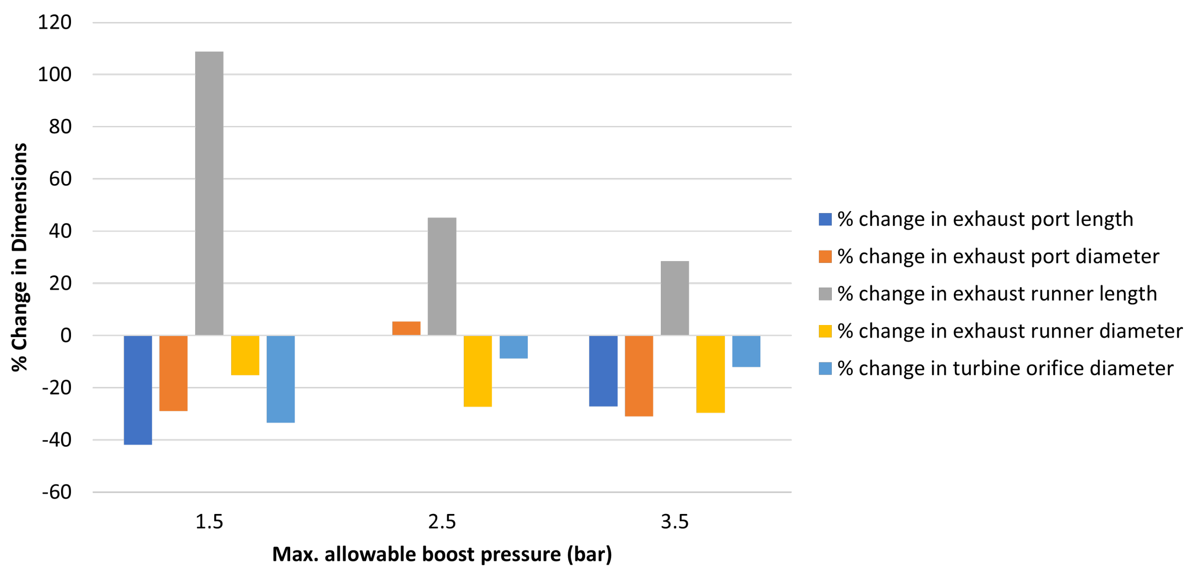

Figure 24: Change in Exhaust Dimensions v/s Boost Pressure Limit

From figure 24, it can be inferred that the EPTE model exhibited the least modification for the exhaust runner length at 3.5 bar maximum boost pressure. Furthermore, it was deduced that at 3.5 bar boost pressure limit, the EPTE could be made compact compared to the baseline engine in relation to other exhaust geometrical variables such as exhaust port length, exhaust port diameter, exhaust runner diameter and turbine orifice diameter while producing the benefits discussed in section 4.1. It must be noted that after the optimization of both the engine models, it was shown that EPTE could operate with the same exhaust port length as that of the baseline engine. Therefore, the ”dark blue” bar is not visible at 2.5 bar maximum allowable boost pressure in figure 24.

4.5 Normalized Brake Torque

The motive behind analyzing the normalized brake torque was to assess if the EPTE model contributed towards the torque fluctuation suppression to a certain degree, when compared against the baseline engine model. The theory related to torque fluctuation in an ICE has been discussed in section 2.2. Such an analysis would help to compare the weight and sizing of flywheel required for both the engines from a qualitative perspective. It must be noted that the engine models simulated in GT-Power^{TM} had no cranktrain inertia object in the part *EngineCranktrain*. This indicated that the flywheel was modelled neither in the baseline engine or the EPTE model. This also provided a foundation to perform a fair comparative analysis for visualizing the effect of both the engine models on the flywheel sizing from a qualitative standpoint.

Figure 25 depicts the variation of normalized brake torque as a function of crank angle degrees. Based on section 4.1, the maximum benefit with the EPTE model was observed at 3.5 bar boost pressure limit and an engine speed of 4500 RPM. Therefore, the graph was extracted for both the engine models operating at a maximum allowable boost pressure of 3.5 bar and the operating engine speed corresponding to figure 25 was 4500 RPM. As per section 4.1, both the engine models had different power output levels throughout the operating speed range. This indicated that the average torque values at a specific engine speed for both the baseline engine and EPTE were different from each other. Therefore, in order to facilitate a fair comparison between the two, it was vital to normalize the instantaneous torque values of both the engine models. For any engine, the normalized brake torque was calculated by dividing the instantaneous torque by the average torque value at that operating engine speed. Figure 25 has been depicted and discussed in the succeeding page.

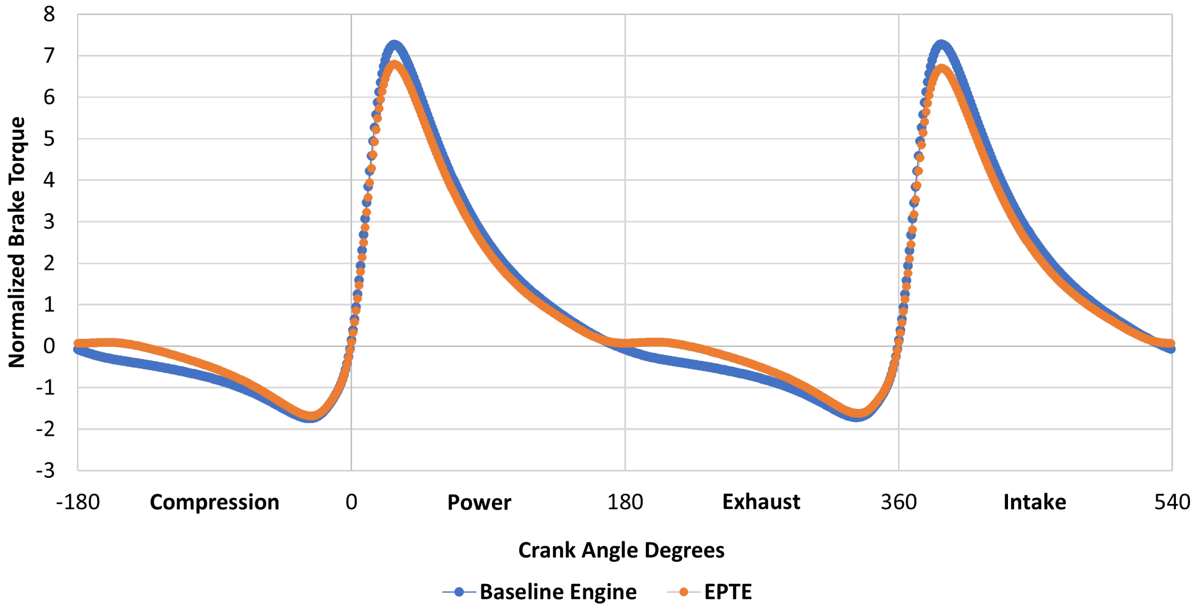

Figure 25: Comparison of Crank-Resolved Normalized Brake Torque

From figure 25, it can be inferred that the fluctuation in the normalized brake torque for the EPTE model was lesser compared to that of the baseline engine model at 3.5 bar maximum allowable boost pressure and 4500 RPM. In this analysis, peak-to-peak difference was considered as an indicator for measuring the fluctuation in normalized brake torque. The reduction in this peak-to-peak difference was observed to be around 6 % relative to the baseline engine model. In section 2.2, it was discussed that lower fluctuations in torque indicates that a flywheel of lower moment of inertia could be attached to the engine crankshaft. Therefore, it was deduced that the EPTE has the potential to be operated with a lighter and more compact flywheel, when compared to the baseline engine.

Chapter 5

Conclusions

This chapter summarizes the results discussed in chapter 4, and thereby provides answers to the research questions listed in chapter 1. It further proposes some recommendations for future work which would foster the development process of the EPTE.

5.1 Discussion

This section summarizes the results emanating from the concept assessment performed in the thesis project. With this, the benefits and drawbacks of the EPTE concept can be visualized based on a system-level simulation approach.

5.1.1 Fuel economy

The EPTE concept proved to be more fuel efficient than the conventional turbocharged ICE topology at high boost pressure limits. However, the new concept exhibited higher fuel consumption values for low boost pressure limit of 1.5 bar, mostly at the higher RPM. The EPTE concept proved to be 4% more fuel efficient on average with 2.5 bar maximum allowable boost pressure, and 5% more fuel efficient on average with 3.5 bar maximum allowable boost pressure.

5.1.2 Power output and EXC's contribution to brake power

The EPTE concept had lower BP levels compared to the baseline engine at 1.5 bar boost pressure limit. This downside came with around 5% reduction on average across the operating range. However, with higher boost pressure limit i.e. at 3.5 bar, the EPTE concept proved to deliver around 4% higher BP on average, when compared with the baseline engine. The EXC component in the EPTE concept contributed to the total BP produced at the crankshaft due to the exhaust gases driving the exhaust piston. It was observed that the EXC component contributed to around 7% of the total BP at 4500 RPM when the boost pressure limit was set to 3.5 bar.

5.1.3 Impact on turbocharger efficiency

The EPTE concept proved to improve the efficiency of the turbocharger with the help of the EXC component, as per figure 18 This is because the EXC component helped in evening out the exhaust pressure into the turbine inlet, which ensured a more even power distribution to the turbine across the whole engine cycle, as compared to the baseline engine.

5.1.4 Impact on muffler and aftertreatment sizing

The EPTE concept proved that a more light-weight and compact muffler and aftertreatment system could be integrated with the engine. This conclusion emanates from the analysis based on figure 19. The EXC component helps in reducing the ”peaks” and ”flutters” in the exhaust pressure measured at the turbine outlet. From this analysis it was inferred that the sizing of exhaust regulation components like muffler and aftertreatment system could be reduced to a suitable level, thereby achieving more compactness in the overall system.

5.1.5 Hardware modifications

Based on the analysis from section 4.4, it was concluded that the EPTE concept can produce the benefits from the fuel economy and power output standpoint, while not having the need to modify the intake and exhaust geometry radically. At boost pressure limit of 3.5 bar, the EPTE concept needed the least modification in exhaust runner length. Whereas, other exhaust geometrical parameters can be made more compact compared to the baseline engine. From the intake side modification standpoint, the EPTE needed around 10 % increment in the runner length and no modification in the runner diameter to produce benefits from the BSFC and BP perspective.

5.1.6 Impact on flywheel inertia

The EPTE concept proved that a more compact and light-weight flywheel could be used in such an engine. This conclusion is based on figure 25. From this analysis, the peak-to-peak reduction in brake torque level was observed to be around 6%, when compared to the baseline engine. This proved that the fluctuations in the torque level is lower and therefore a lower inertia flywheel could be integrated with the EPTE concept. Thanks to the EXC component.

5.2 Recommendations

Based on the overall modelling and analysis process, the EPTE concept proved to have higher benefits than the conventional turbocharged ICE topology from both fuel consumption and power output standpoint. These benefits were observed for high boost pressure limits. Therefore to foster and accelerate the development of the EPTE concept, it would be recommended to assess such a concept for turbocharged engines operating at high boost pressures. Diesel engines for heavy-duty applications and large-bore 4-stroke marine engines fall under this category. Assessing the potential of this concept for these pre-existing engine models can help to realize the benefits of the EPTE concept on a broader level. Another recommendation would be to perform an assessment on existing turbocharged engines for which performance maps are available for both the turbine and compressor components. This will help to assess the turbocharger efficiency enhancement with better resolution across the relevant operating speed range. Thirdly, a semi-predictive combustion model could be used while analyzing the impact of EXC component on the performance and gas exchange metrics of the overall engine system. This would mean that the combustion rate of air-fuel mixture would be influenced by other input variables based on look-up tables. It offers a good balance between predictive and non-predictive combustion modelling from the internal validity standpoint [10]. These studies will be crucial before commencing hardware development activities.

References

[1] Branyon, David. and Simpson, Dean. “Miller Cycle Application to the Scuderi Split Cycle Engine (by Downsizing the Compressor Cylinder)”. In: *SAE 2012 World Congress Exhibition*. SAE International, Apr. 2012. DOI: https://doi.org/10.4271/2012-01-0419. URL: https://doi.org/10.4271/2012-01-0419.

[2] Bumby, J.R., Spooner, E.S., Carter, J., Tennant, H., Mego, G.G., Dellora, G., Gstrein, W., Sutter, H., and Wagner, J. “Electrical machines for use in electrically assisted turbochargers”. In: *Second International Conference on Power Electronics, Machines and Drives (PEMD 2004)*. Vol. 1. 2004, 344–349 Vol.1. DOI: 10.1049/cp:20040310.

[3] Chen, Simon K. and Flynn, Patrick F. *Development of a Single Cylinder Compression Ignition Research Engine*. eng. SAE Technical Paper Series. 1965.

[4] Colin, Guillaume., Chamaillard, Yann., and Bellicaud, Benoit. “Robust control for the air path of a downsized engine”. In: *Proceedings of the Institution of Mechanical Engineers, Part D: Journal of Automobile Engineering* 225 (July 2011), pp. 930–943. DOI: 10.1177/0954407011401503.

[5] Dijkstra, Rutger., Boot, Michael., Eichhorn, Ruud., Smeulders, D., Lennblad, Johan., and Serrarens, Alex. “Experimental Analysis of Engine Exhaust Waste Energy Recovery Using Power Turbine Technology for Light Duty Application”. In: *SAE International Journal of Engines* 5 (Jan. 2012), pp. 1729–1739. DOI: 10.4271/2012-01-1749.

[6] *Draft Technical Assessment Report: Midterm Evaluation of Light-Duty Vehicle Greenhouse Gas Emission Standards and Corporate Average Fuel Economy Standards for Model Years 2022-2025*. Tech. rep. EPA, CARB, 2016. URL: https://nepis.epa.gov/Exe/ZyPDF.cgi/P100OXEO.PDF?Dockey=P100OXEO.PDF.

[7] Ebisu, M., Danmoto, Y., Akiyama, Y., Arimizu, H., and Sakamoto, K. *Development of Variable Geometry Turbocharger Contributes to Improvement of Gasoline Engine Fuel Economy*. Tech. rep. Mitsubishi Heavy Industries Technical Review Vol. 53 No.3, Sept.

2016. DOI: https://www.mhi.co.jp/technology/review/pdf/e533/e533030.pdf.

[8] Ferrara, Michael. *Twin Scroll vs. Single Scroll Turbo Test | The Great Divide*. 2016-02-29. URL: https://dsportmag.com/the-tech/twin-scroll-vs-single-scroll-turbo-test-the-great-divide/ (visited on 08/17/2021).

[9] Gamma Technologies, 2019. *ENGINE (GT-POWER) COMPONENTS : IntercoolerEff - Intercooler Outlet Gas Temperature Control*. Available in the template help for 'IntercoolerEff'. Last accessed 30/08/2021. Westmont, IL, 2019.

[10] Gamma Technologies, 2019. *Engine Performance Application Manual Version 2019*. Last accessed 25/08/2021. Westmont, IL, 2019.

[11] Gamma Technologies, 2019. *Flow Theory Manual Version 2019*. Last accessed 25/08/2021. Westmont, IL, 2019.

[12] Gamma Technologies, 2019. *Optimization Manual Version 2019*. Last accessed 01/09/2021. Westmont, IL, 2019.

[13] Gamma Technologies, 2019. *TURBINES, PUMPS AND COMPRESSORS COMPONENTS: CompressorSimple - Simple Compressor if No Map Data Available*. Available in the template help for 'CompressorSimple'. Last accessed 01/09/2021. Westmont, IL, 2019.

[14] Gamma Technologies, 2019. *TURBINES, PUMPS AND COMPRESSORS COMPONENTS: TurbineSimple - Simple Turbine if No Map Data Available*. Available in the template help for 'TurbineSimple'. Last accessed 01/09/2021. Westmont, IL, 2019.

[15] *GT-POWER Engine Simulation Software*. 2015. URL: https://www.gtisoft.com/wp-content/uploads/2015/01/Power1.pdf (visited on 08/24/2021).

[16] Heywood, John B. "ENGINE OPERATING CYCLES". en. In: *Internal Combustion Engine Fundamentals, Second Edition*. 2nd edition. New York: McGraw-Hill Education, 2018. ISBN: 9781260116106. URL: https://www.accessengineeringlibrary.com/content/book/9781260116106/toc-chapter/chapter1/section/section4.

[17] Heywood, John B. “INTRODUCTION AND HISTORICAL PERSPECTIVE”. en. In: *Internal Combustion Engine Fundamentals, Second Edition*. 2nd edition. New York: McGraw-Hill Education, 2018. ISBN: 9781260116106. URL: https://www.accessengineeringlibrary.com/content/book/9781260116106/toc-chapter/chapter1/section/section2.

[18] Heywood, John B. “SUPERCHARGING AND TURBOCHARGING”. en. In: *Internal Combustion Engine Fundamentals, Second Edition*. 2nd edition. New York: McGraw-Hill Education, 2018. ISBN: 9781260116106. URL: https://www.accessengineeringlibrary.com/content/book/9781260116106/toc-chapter/chapter6/section/section47.

[19] Ishii, Mori., Shimokawa, Kiyohiro., Machida, Koichi., and Nakajima, Hiroshi. “A Study on Improving Fuel Consumption of Heavy-Duty Diesel Engine Specifically Designed for Long-Haul Trucks on Highway”. In: Apr. 2015. DOI: 10.4271/2015-01-1256.

[20] Jääskeläinen, Hannu. *Miller Cycle Engines*. 2019-12-04. URL: https://dieselnet.com/tech/engine_miller-cycle.php#early-late (visited on 08/17/2021).

[21] Kim, SeHwan. and Seok, Jul-Ki. “Comprehensive PM motor controller design for electrically assisted turbo-charger systems”. In: *2013 IEEE Energy Conversion Congress and Exposition*. 2013, pp. 860–866. DOI: 10.1109/ECCE.2013.6646793.

[22] Lee, Woongkul., Schubert, Erik., Li, Yingjie., Li, Silong., Bobba, Dheeraj., and Sarlioglu, Bulent. “Overview of Electric Turbocharger and Supercharger for Downsized Internal Combustion Engines”. In: *IEEE Transactions on Transportation Electrification* 3 (Mar. 2017), pp. 36–47. DOI: 10.1109/TTE.2016.2620172.

[23] Miller, Ralph. *Supercharged engine. patent US2817322A*. 1957-12-24. URL: https://patents.google.com/patent/US2817322A/en.

[24] Nhut, Lam. “Double Compression-Expansion Engine Concepts: Experimental and simulation study of a split-cycle concept for improved brake efficiency”. English. Defence details Date: 2019-05-03 Time: 10:15 Place: Lecture Hall M:B, M-Building, Ole Römers väg 1, Lund University, Faculty of Engineering LTH External reviewer(s) Name: Morgan, Robert Title: Professor Affiliation: University of Brighton, United Kingdom —. PhD thesis. 2019. ISBN: 978-91-7895-050-8.

[25] Nikuradse, J. *Strömungsgesetze in rauhen Rohren*. Forschungsheft. Beilage zu “Forschung auf dem Gebiete des Ingenieurwesens”. Ausgabe B Band 4, Juli-August 1933 ; VDI-Verlag, 1933.

[26] Noga, Marcin. "Five-stroke Internal Combustion Engine - yesterday, today and tomorrow". In: *IOP Conference Series: Materials Science and Engineering* 421 (Oct. 2018), p. 042058. DOI: 10.1088/1757-899X/421/4/042058.

[27] Olshammar, Mats. *Internal Combustion Engine with Turbocharge Arrangement*. 2019. URL: https://patents.google.com/patent/WO2019078776A1/en.

[28] Olsson, Viktor. *An on-engine twin-scroll turbine performance estimation*. 2015. URL: http://urn.kb.se/resolve?urn=urn:nbn:se:kth:diva-170801.

[29] Ratnaweera, Asanga. *Design of a Flywheel*. URL: http://eng.pdn.ac.lk/old/mechanical/menu/class/downloads/notes/flywheel_ppt.pdf.

[30] Romagnoli, Alessandro., Copeland, Colin D., Martinez-Botas, Ricardo., Seiler, Martin., Rajoo, Srithar., and Costall, Aaron. "Comparison Between the Steady Performance of Double-Entry and Twin-Entry Turbocharger Turbines". In: *Journal of Turbomachinery* 135.1 (Oct. 2012). 011042. ISSN: 0889-504X. DOI: 10.1115/1.4006566. eprint: https://asmedigitalcollection.asme.org/turbomachinery/article-pdf/135/1/011042/6296719/turb_135_1_011042.pdf. URL: https://doi.org/10.1115/1.4006566.

[31] Schmitz, Gerhard. *Five-stroke internal combustion engine, Patent US6553977B2*. 2003-04-29. URL: https://patents.google.com/patent/US6553977B2/en.

[32] Schutting, Eberhard., Dumböck, Ortwin., Kraxner, Thomas., and Eichlseder, Helmut. "Thermodynamic consideration of the Miller cycle on the basis of simulation and measurements". In: *Internationaler Motorenkongress 2016*. Ed. by Johannes. Liebl and Christian. Beidl. Wiesbaden: Springer Fachmedien Wiesbaden, 2016, pp. 259–280. ISBN: 978-3-658-12918-7.

[33] Shahed, S. and Bauer, Karl-Heinz. "Parametric Studies of the Impact of Turbocharging on Gasoline Engine Downsizing". In: *SAE International Journal of Engines* 2 (Oct. 2009), pp. 1347–1358. DOI: 10.4271/2009-01-1472.

[34] Silva Cardoso, D., Oliveira Fael, P., and Espírito-Santo, A. "Instantaneous angular velocity and torque on Otto single-cylinder engine: A theoretical and experimental analysis". In: *Energy Reports* 6 (2020). The 7th International Conference on Energy and Environment Research—"Driving Energy and Environment in 2020 Towards A Sustainable Future", pp. 43–48. ISSN: 2352-4847. DOI: https://doi.org/10.1016/j.egyr.2020.10.031. URL: https://www.sciencedirect.com/science/article/pii/S2352484720313846.

[35] Subramani, DA., Dhinagaran, R., and Prasanth, VR. "Introduction to turbocharging—a perspective on air management system". In: *Design and Development of Heavy Duty Diesel Engines*. Springer, 2020, pp. 85–193.

[36] *Twin-scroll turbochargers*. URL: `https://x-engineer.org/automotive-engineering/internal-combustion-engines/ice-components-systems/twin-scroll-turbochargers/` (visited on 08/12/2021).

[37] Uhlmanna, Tolga., Lückmannb, Dominik., Aymannsa, Richard., Scharf, Johannes., Höpkeb, Björn., Scassac, Mauro., Rüttena, Oliver., Schornd, Norbert., and Kindld, Helmut. "DEVELOPMENT AND MATCHING OF DOUBLE ENTRY TURBINES FOR THE NEXT GENERATION OF HIGHLY BOOSTED GASOLINE ENGINES". In: 2014.

[38] Venkataraman, V. "The Miller Cycle on Single-Cylinder and Serial Configurations of a Heavy-Duty Engine". In: 2018. URL: `https://kth.diva-portal.org/smash/get/diva2:1196111/FULLTEXT01.pdf`.

[39] Wu, Chih., Puzinauskas, Paul V., and Tsai, Jung S. "Performance analysis and optimization of a supercharged Miller cycle Otto engine". In: *Applied Thermal Engineering* 23.5 (2003), pp. 511–521. ISSN: 1359-4311. DOI: `https://doi.org/10.1016/S1359-4311(02)00239-9`. URL: `https://www.sciencedirect.com/science/article/pii/S1359431102002399`.

Appendix A

GT-Power™ Modelling

Appendix A deals with additional GT-Power^{TM} modelling theories required to understand the methodology better along with enlarged views of baseline engine and EPTE models.

A.1 Modelling Theory

This section explains additional theory regarding time step calculation and split flow modelling briefly mentioned in subsections 3.3.1 and 3.4.1. All equations in this section are derived from GT-Power^{TM} documentation files [10, 11].

Time step calculation

Courant condition specifies the condition that must be satisfied to achieve convergence while solving flow equations like the Navier-Stokes equations in explicit method. the time step must be chosen in such a way that it satisfies the Courant condition in order to achieve numerical stability. The Courant number, C, is a dimensionless number that establishes the relation between time step and discretization length [11]. The Courant condition is given by:

$$\frac{\Delta t}{\Delta x}(|u| + c) \leq C * m \tag{A.1}$$

We can get the equation A.2 for time step by rearranging the equation A.1 and removing the inequality.

$$\Delta t = \frac{C * M * \Delta x}{|u| + c} \tag{A.2}$$

where, Δt is the time step (s), Δx is the minimum discretization length of the element (m), u is the fluid velocity (m/-s), c is the speed of sound (m/s) and M is the time step multiplier specified by the user in RunSetup (less than or equal to 1.25).

The value of C should be equal to or less than 1.0. GT-Power^{TM} uses a value $C = 0.8$ to make sure that a wide range of models can attain solution stability [11].

Split flow modelling

The flow solver in GT-Power^{TM} provides a one-dimensional solution of the Navier-Stokes equation. At the centers of finite volumes, mass and energy equations (scalar) are calculated, while mass flow equation (vector) are solved at the boundaries between them. A flowsplit is formed when a finite volume has several entrances. Friction and heat transfer solutions are computed in the same way that pipes are. The key distinction is that the velocities used in calculating friction and heat transfer coefficients are weighted boundary velocities [11].

In this thesis, *FlowSplitTRight* object was used. This object has three boundaries, with one pipe being perpendicular to the other two pipes, resembling the shape of 'T'. This object is a simplified way of modelling a pipe that intersects with another pipe at right angles. This flowsplit is defined in the same way that a pipe is, with only the main diameter and length of the flowsplit required to define the flowsplit geometry. The boundary geometry is known from the *FlowSplitTRight* object's default geometry as well as the associated orifices and pipes. Figure 26 depicts the *FlowSplitTRight* object, where dx is the discretization length and D is the internal expansion diameter of boundaries 1 and 2 [11].

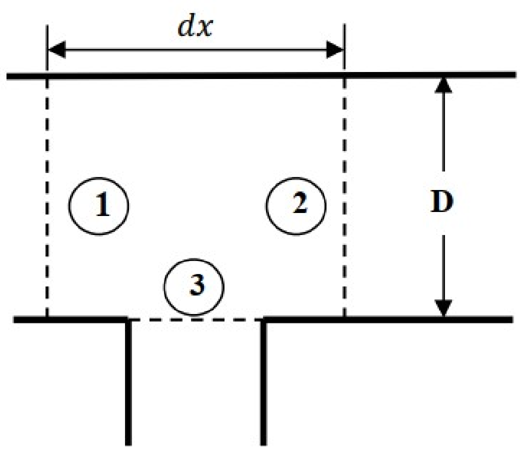

Figure 26: *FlowSplitTRight* object [11]

A.2 Baseline engine & EPTE models - Enlarged view

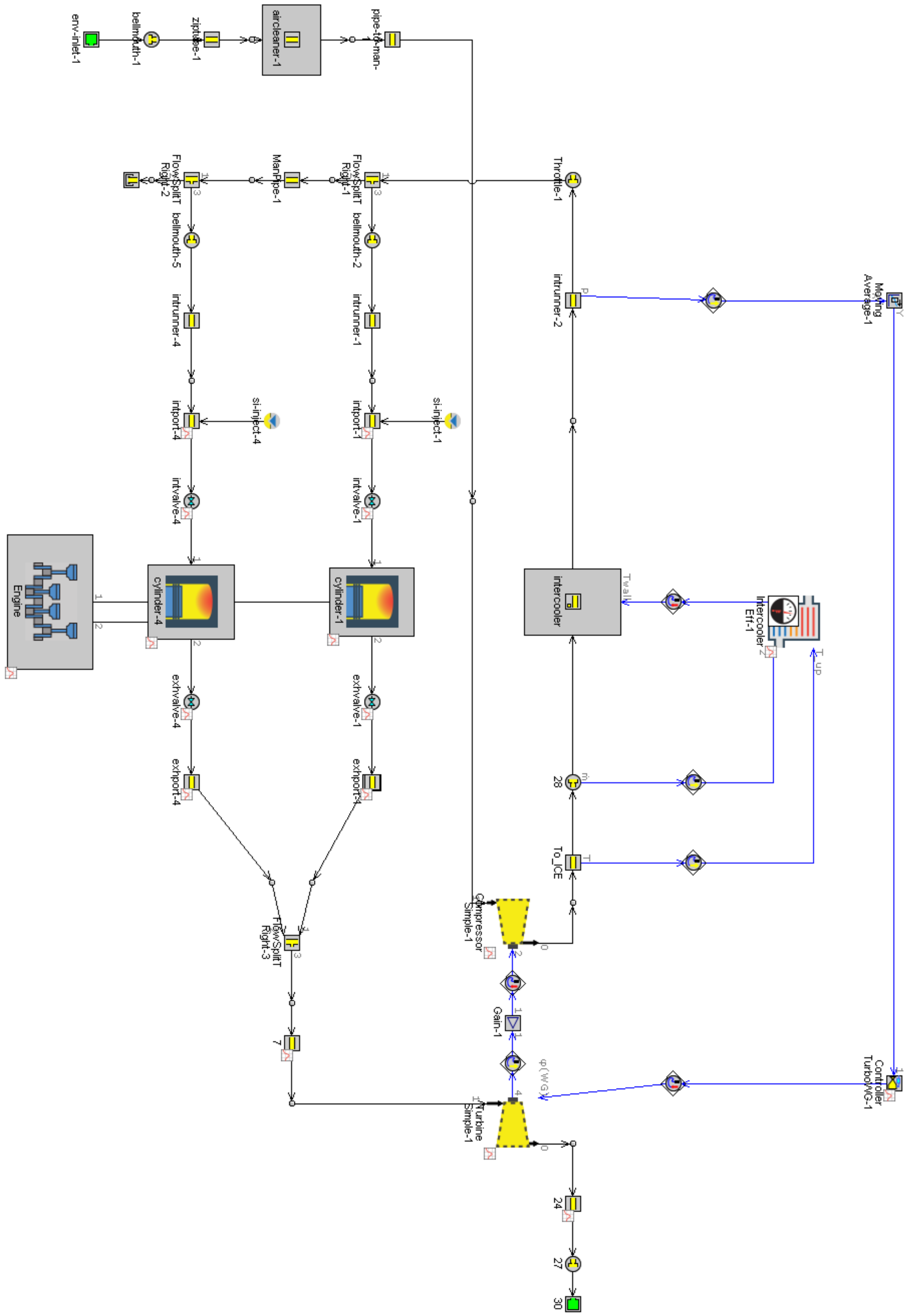

Figure 27: Baseline Engine Model - Enlarged View

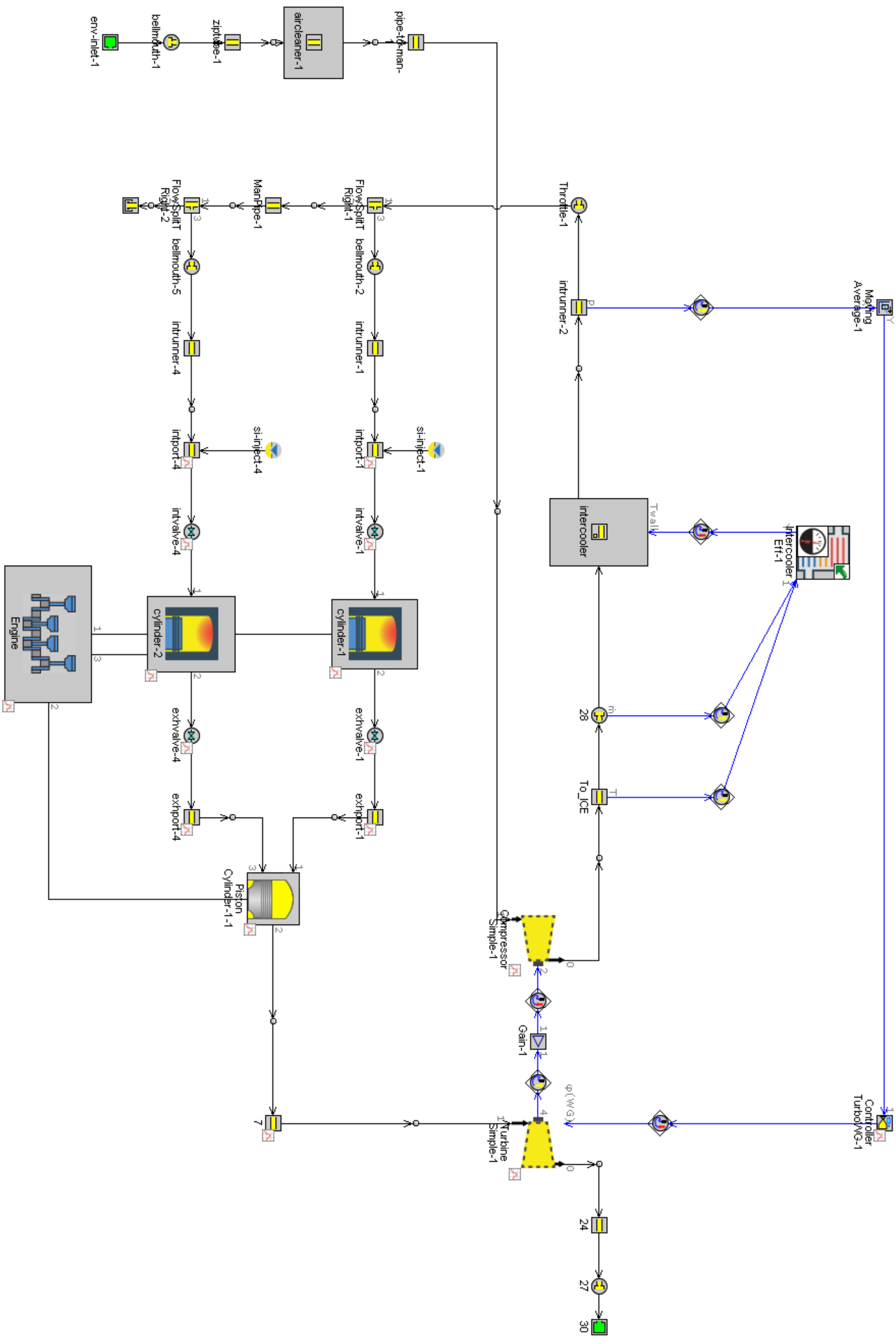

Figure 28: EPTE model - Enlarged View

Appendix B

Miscellaneous Results

This particular appendix deals with the results related to the optimized specifications of the EXC component which were not explained in chapter 4, but would be interesting for the reader to understand the EPTE model results with more clarity. It also gives an overview on how the DOE studies were performed, using a specific example.

B.1 EXC Specifications - Post Optimization

This section discusses the specifications of the EXC component in the EPTE model after the optimization was performed. The motive of discussing this section is to give an understanding of the changes required in the EXC component relative to the combustion cylinders, when producing the benefits from the performance metric standpoint as discussed in section 4.1. It must be noted that the specifications are shown for 2.5 bar and 3.5 bar maximum allowable boost pressures as the benefits from the fuel consumption and power output standpoint were observed at these operating conditions. Figure 29 depicts the component in GT-Power™ modelling context. The modelling approach for EXC is described in subsection 3.4.2.

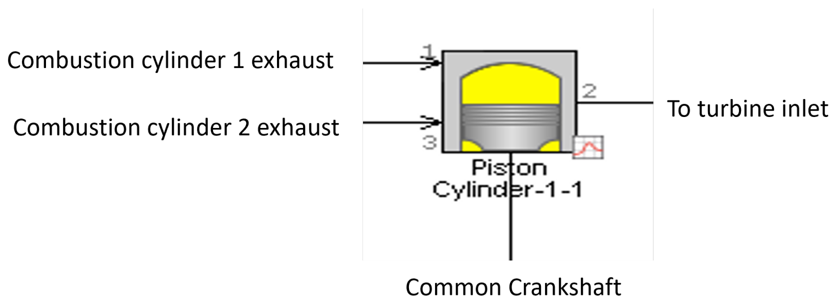

Figure 29: EXC Component in GT-Power™

The component has the following features:

1. It is placed in between the two combustion cylinders.
2. It is connected to the same crankshaft as that of the combustion cylinders.
3. Since the EXC component is placed on a common crankshaft, it has the same stroke length as that of the combustion cylinders.
4. There is no combustion occurring inside.
5. There are no valves inside the EXC component.
6. Since there are no valves inside, the EXC component can have a different compression ratio compared to that of the combustion cylinders. Absence of valves prevents high pressure build up, even if the compression ratio is high.

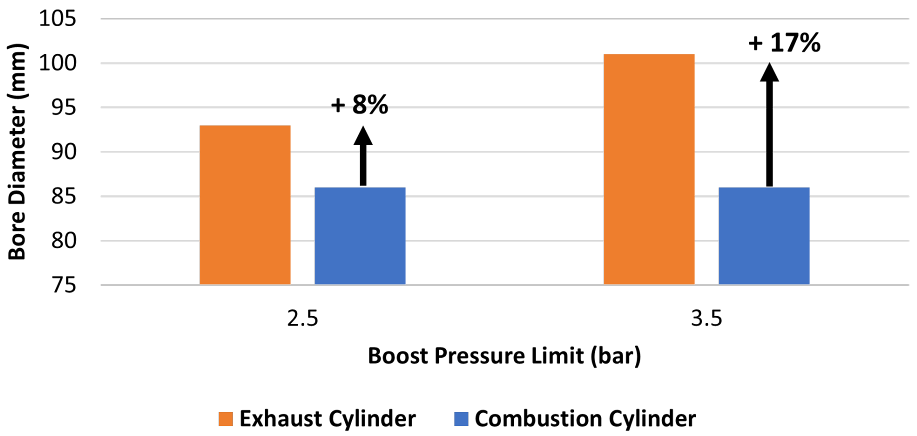

(a) Bore Diameter Comparison - EXC and Combustion Cylinder

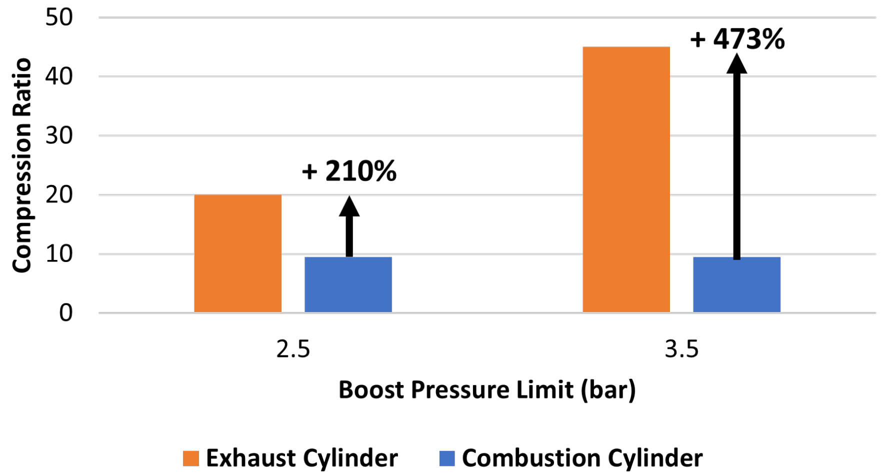

(b) Compression Ratio Comparison - EXC and Combustion Cylinder

Figure 30: EXC Specifications - Post Optimization

Figure 30 shows the comparison of cylinder bore diameter and geometrical compression ratio between the EXC component and the combustion cylinder. After the optimization for the EPTE model was performed, these geometrical characteristics were compared. From figure 30, it was inferred that the EXC component needs to be wider compared to the combustion cylinder, while maintaining the same stroke length. Furthermore, higher geometrical compression ratio is required compared to the combustion cylinder. It must be noted that the absence of valves and combustion inside the EXC component would help in achieving higher geometrical compression ratio relative to the combustion cylinder.

B.2 Design of Experiments (DOE)

As mentioned in section 3.5, DOE studies were performed before the commencement of the model optimization process. The motive behind performing DOE studies was to understand the behaviour of the baseline engine and EPTE models from the BSFC and BP standpoint, under the influence of various engine variables. Furthermore, the studies were also useful in identifying a suitable range for the engine variables, which was later deployed in IDO during the optimization process as per tables 11 and 12.

The DOE studies performed were based on an iterative approach. In a DOE study, the influence of two engine variables on BSFC and BP were analyzed, while keeping all other factors constant. While performing a DOE study, a range for both the input variables were considered along with a specified interval size. After the analysis, the range and interval size of the input variables were changed to accommodate the resolution demands of the study, if needed. All the DOE studies were based on a full-factorial method i.e., every possible combination of both the input variables within the specified range was analyzed to understand the response of both the engine models from the BP and BSFC perspective. The most suitable combination of the two input variables were then chosen which yielded maximum BP and minimum BSFC across the operating engine RPM range. This combination was further used in the subsequent DOE study which involved a combination of other engine variables.

Since it was not possible to include all the DOE results in this report because of its iterative nature, an example has been depicted which would help in understanding on how this process was performed. Figures 31 and 32 have been represented in the following page to serve as an example.

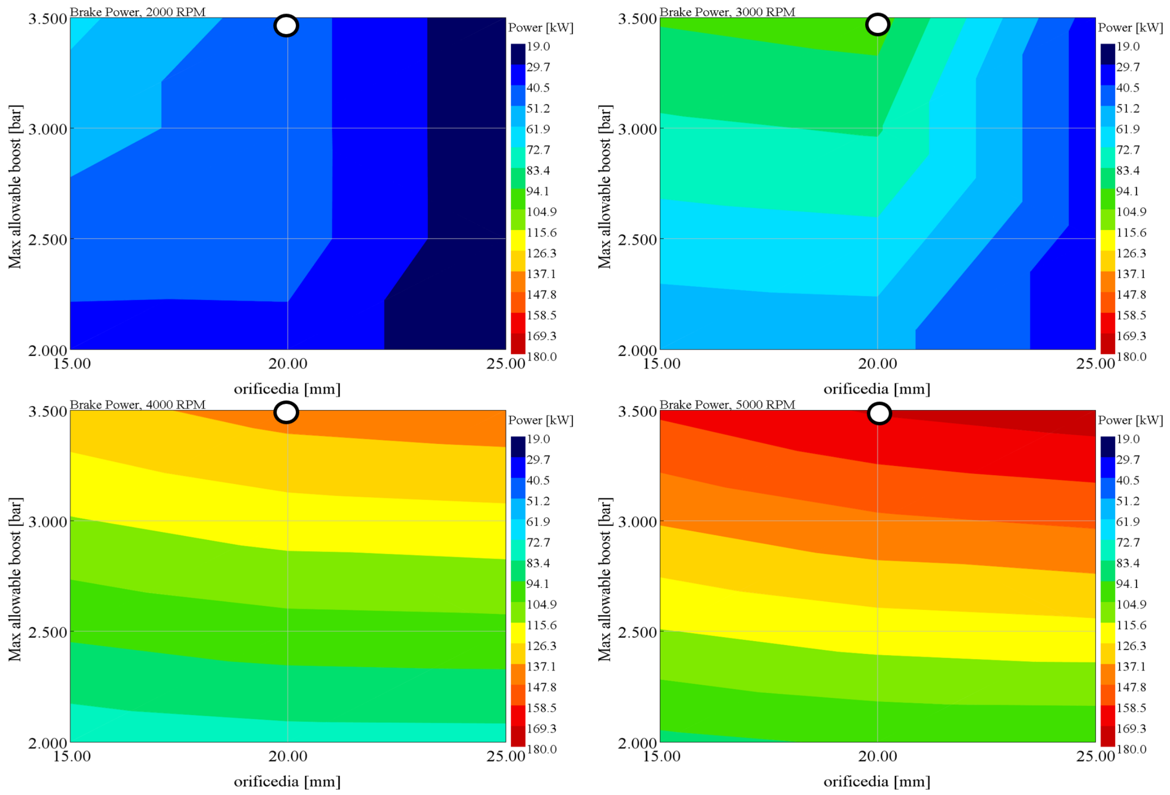

Figure 31: DOE Plots for BP - Turbine Orifice Diameter & Max. Allowable Boost Pressure

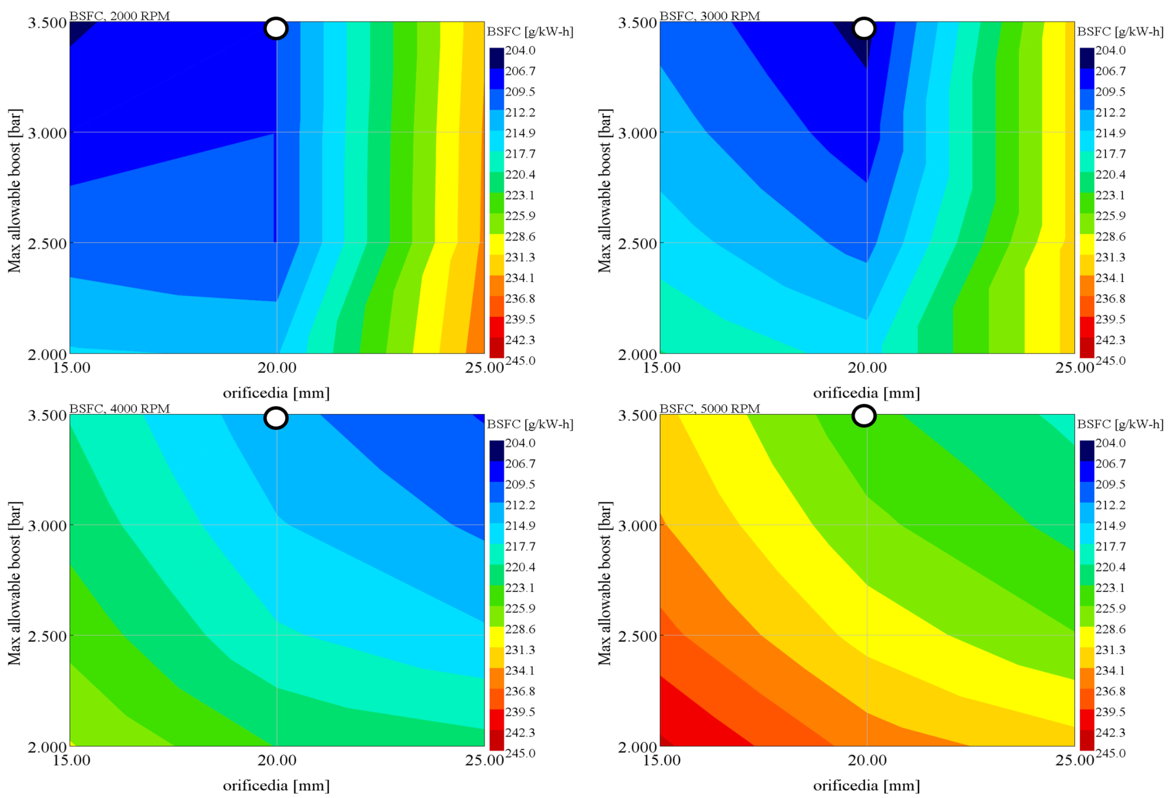

Figure 32: DOE Plots for BSFC - Turbine Orifice Diameter & Max. Allowable Boost Pressure

Figures 31 and 32 depict one of the DOE-based simulations performed before the optimization process. These figures capture the BP and BSFC of the EPTE model under the influence of a range of turbine orifice diameters, and maximum allowable boost pressures regulated by the wastegate of the turbocharger. All other factors related to the engine model within the particular DOE-based simulation were kept constant. The plots are shown for 2000, 3000, 4000 and 5000 RPM within the considered range of 2000 RPM to 6500 RPM. The x-axis and y-axis values represent the tested points in the DOE study. The plots implied that the most suitable combination which yielded maximum power output and best fuel economy across the engine RPM range, was 20 mm turbine orifice diameter at 3.5 bar max. allowable boost pressure. This combination, represented in white circles, was then used as a constant input factor for the subsequent DOE study. The process continued until the engine models were visualized on a system-level, and a reasonable range of engine variables was decided for the optimization process to provide a more accurate and fair platform for the comparison of baseline engine and EPTE models.

TRITA-ITM-EX 2021:546